Kurano et al. Lipids in Health and Disease 2011, 10:134
http://www.lipidworld.com/content/10/1/134

LIPIDS IN HEALTH AND DISEASE

RESEARCH Open Access

LXR agonist increases apoE secretion from HepG2 spheroid, together with an increased production of VLDL and apoE-rich large HDL

Makoto Kurano[1], Naoyuki Iso-O[5], Masumi Hara[5], Nobukazu Ishizaka[2], Kyoji Moriya[3], Kazuhiko Koike[4] and Kazuhisa Tsukamoto[1,7*]

Abstract

Background: The physiological regulation of hepatic apoE gene has not been clarified, although the expression of apoE in adipocytes and macrophages has been known to be regulated by LXR.

Methods and Results: We investigated the effect of TO901317, a LXR agonist, on hepatic apoE production utilizing HepG2 cells cultured in spheroid form, known to be more differentiated than HepG2 cells in monolayer culture. Spheroid HepG2 cells were prepared in alginate-beads. The secretions of albumin, apoE and apoA-I from spheroid HepG2 cells were significantly increased compared to those from monolayer HepG2 cells, and these increases were accompanied by increased mRNA levels of apoE and apoA-I. Several nuclear receptors including LXRα also became abundant in nuclear fractions in spheroid HepG2 cells. Treatment with TO901317 significantly increased apoE protein secretion from spheroid HepG2 cells, which was also associated with the increased expression of apoE mRNA. Separation of the media with FPLC revealed that the production of apoE-rich large HDL particles were enhanced even at low concentration of TO901317, and at higher concentration of TO901317, production of VLDL particles increased as well.

Conclusions: LXR activation enhanced the expression of hepatic apoE, together with the alteration of lipoprotein particles produced from the differentiated hepatocyte-derived cells. HepG2 spheroids might serve as a good model of well-differentiated human hepatocytes for future investigations of hepatic lipid metabolism.

Keywords: Spheroid HepG2 cells, LXR agonist, Apolipoprotein E, ApoE rich HDL, VLDL

Background

Apolipoprotein E (apoE), a 34-kD glycoprotein produced mainly by hepatocytes and also secreted from several cells including macrophages and adipocytes, plays a crucial role in lipoprotein metabolism and atherosclerosis. It mediates the cellular uptake of several classes of lipoproteins by acting as a ligand for the chylomicron remnant receptor, the VLDL receptor, LDL receptor and the LDL receptor-related protein (LRP). ApoE produced by macrophages and those accessing macrophages from the bloodstream facilitate the reverse cholesterol transport by promoting the formation and maturation of HDL particles [1,2]. In addition to these functions, apoE produced in hepatocytes enhances the production of VLDL particles [3]. The increased production of hepatic VLDL particles, a phenomenon observed in insulin-resistant patients or some primary hyperlipidemia subjects, leads to the accumulation of atherogenic lipoproteins in the circulation resulting in the aggravation of atherosclerosis.

The genetic regulation of the apoE gene has been pursued extensively. Taylor et al has identified two hepatic enhancer elements located far-downstream of the apoE gene, and clarified the regions critical to the baseline expression of the apoE gene [4,5]. They also identified the duplicated downstream enhancer elements termed multienhancers (ME.1 and ME.2), and demonstrated that these elements are crucial for apoE expression in macrophages and adipocytes [6]. In addition, Laffitte

* Correspondence: kazuhisa-tky@umin.ac.jp
[1]Department of Metabolic Diseases, Graduate School of Medicine, The University of Tokyo, Tokyo 113-8655, Japan
Full list of author information is available at the end of the article

et al elegantly clarified that the nuclear receptor liver × receptor (LXR) regulates apoE expression in adipocytes and macrophages through direct interaction of the LXR response element found in both ME.1 and ME.2 [7].

In spite of these extensive analyses on apoE gene regulation, physiological factors which affect gene regulation of apoE in the liver have not been elucidated so far. Previous in vivo studies utilizing guinea pig [8] and cebus monkey [9] have shown that cholesterol feeding to these animals resulted in the up-regulation of apoE gene in the liver, raising the possibility that the accumulation of cholesterol in hepatocytes would affect hepatic up-regulation of the apoE gene. In addition, investigation in mice also indicated the up-regulation of hepatic apoE gene by cholesterol feeding [10]. However, the contribution of LXR in the regulation of murine hepatic apoE was not demonstrated [7,10]. Furthermore, no study has clarified the role of LXR in the regulation of hepatic apoE gene in human-derived hepatocytes or hepatic cell lines, with only one exception which utilized artificial reporter gene construct, in which ME.1 or ME.2 was placed just before the -890 to +93 apoE promoter [7].

As for the model of human hepatocytes, HepG2 cells have been widely used for in vitro experiments; however HepG2 cells grown in monolayer form on a culture plate are different from the in vivo hepatocytes which exist in three dimensional form in the liver, and would not completely reflect the physiological functions of hepatocytes. HepG2 cells in spheroid culture, which grow in three dimensional form after being encapsulated in alginate beads [11], have been shown to be more differentiated than HepG2 cells cultured in monolayer form; the cells proliferating in alginate beads form cell-cell contact with each other, and normal hepato-cellular junctional complexes including canaliculi with microvilli are constructed [11]. In consequence, the production of several proteins and the detoxificatory functions [11] as well as the production of cholesterol and triglycerides [12] increased significantly in HepG2 cells in spheroid culture compared to those in monolayer culture.

In this report, we first compared the production of several apolipoproteins from HepG2 cells in spheroid culture with those in monolayer culture. Next, we examined the effect of TO901317, a synthetic LXR ligand, on the secretion of apoE as well as lipoproteins with HepG2 cells cultured both in three-dimensional form and in monolayer form.

Results

HepG2 cells cultured in spheroid form (S-Hep) secreted more albumin and apolipoproteins than HepG2 cells cultured in monolayer (M-Hep)

HepG2 cells cultured in spheroid form grew in three dimensional form (Figure 1A). To validate the differentiation of HepG2 cells prepared as spheroids in our procedure, we first examined the time-course changes in the secretion of albumin. As shown in Figure 1B, the secretion of albumin from S-Hep was enhanced; the highest secretion level was observed on Day 11, reaching as high as 4.5-fold compared to M-Hep, which was concordant with the previous report [11]. The secretions of apolipoprotein A-I (apoA-I), apoE, and apolipoprotein B (apoB) did also increase in S-Hep, and the time-course changes in their levels were almost the same as those found with albumin (Figure 1C-E). The mRNA levels of apoA-I and apoE on Day 11 of S-Hep revealed a 3-fold and 3.5-fold increase compared to M-Hep (Figure 2A). Because the levels of albumin and apoE secretions were highest on Day 11, for the subsequent experiments, we utilized S-Hep on Day 11.

PPAR-α, PPAR-γ, LXR-α, RXR-α were more abundant in the nuclear fractions of S-Hep than in those of M-Hep

In order to elucidate whether the up-regulation of the genes of apolipoproteins in S-Hep were associated with changes in the nuclear receptors, we next examined the nuclear protein levels in S-Hep in comparison with M-Hep. As shown in Figure 2B and 2C, the Western blot analyses of the proteins prepared from nuclear fractions revealed that peroxisome proliferator-activated receptor (PPAR)-α, LXR-α and retinoid × receptor (RXR)-α were more abundant in S-Hep than M-Hep. We did not observe differences in nuclear protein levels of hepatocyte nuclear factor (HNF)1-α and HNF4-α between S-Hep and M-Hep, however, PPAR-γ was also increased in S-Hep. This result suggested that the state of differentiation of hepatic derived cells would affect the expressions of several proteins associated with lipid metabolism at the level of DNA transcription.

TO901317 increased apoE secretion and suppressed apoA-I secretion from HepG2 spheroids more evidently than monolayer HepG2 cells

The increased nuclear level of LXRα in S-Hep together with the increased secretion of apoE from S-Hep prompted us to evaluate the effect of LXRα agonist on the secretion of apoE, because LXRα has been identified as a critical factor for the regulation of apoE in macrophages and adipocytes. Thus we next examined the effect of TO901317 (TO), a synthetic LXRα agonist, on the apolipoproteins' secretion from S-Hep as well as M-Hep. As was shown in Figure 3A, the incubation of cells with TO did not alter the levels of apoB secretion in both S-Hep and M-Hep. The secretion of apoA-I was decreased in both forms of HepG2 cells when the cells were incubated with TO, which was concordant with the previous finding by Huuskonen et al (Figure 3B) [13]. On the other hand, apoE secretion was enhanced

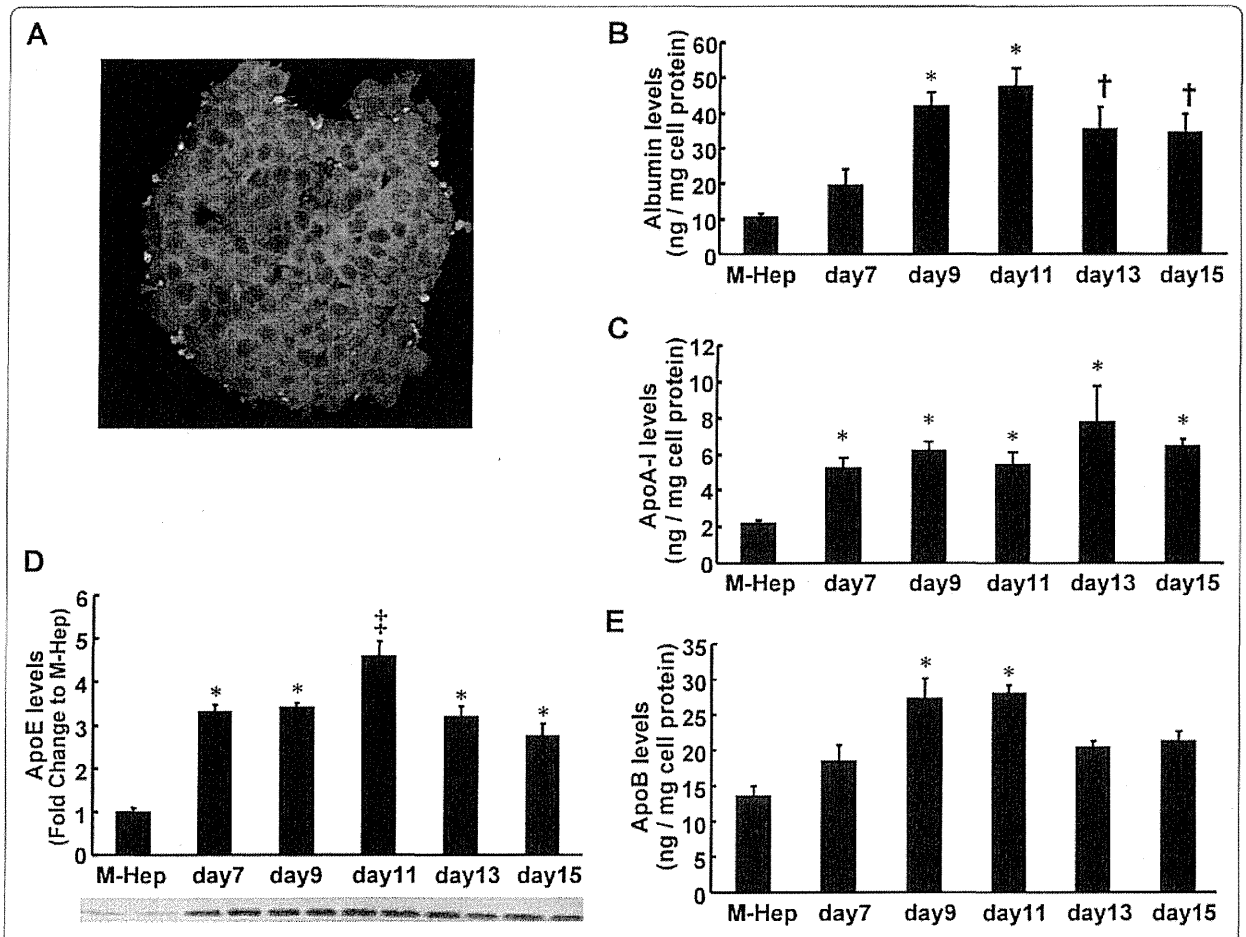

Figure 1 Differences in albumin and apolipoproteins secretion between monolayer and spheroid HepG2 cells. (A) Representative appearance of HepG2 spheroids on Day 11. HepG2 spheroids were fixed with 10% formalin solution, and examined with confocal microscopy. Briefly, from a single HepG2 cell, cells proliferate and form a spheroidal cell-cluster in an aliginate bead. (B-E) Time-course changes in the secretion of albumin (B), apoA-I (C), apoE (D), and apoB (E) from S-Hep cells. S-Hep (spheroid HepG2 cells) were prepared and grown in alginate beads as described in Materials and Methods, and the protein levels in the media on different time points after the beginning of the culture were measured. X axes represent the days after the beginning of S-Hep culture. Data are mean ± SEM (n = 4). *: $P < 0.01$ compared with M-Hep; †: $P < 0.03$ compared with M-Hep; ‡: $P < 0.01$ compared with M-Hep and $P < 0.03$ with S-Hep on the other time points.

not only in S-Hep but also in M-Hep with the incubation of cells with TO (Figure 3C). The induction of apoE in M-Hep plateaued at 0.02 μM TO, while the dose-dependent increase in apoE secretion from S-Hep was observed up to 0.2 μM. In addition, this incremental apoE secretion was more prominent in S-Hep, reaching almost twice the level of cells without TO.

TO901317 increased apoE and ABCA1 mRNA levels in HepG2 spheroids

In order to evaluate whether the increased secretion of apoE from S-Hep treated with TO was associated with the upregulation of the apoE gene, we examined the levels of apoE mRNA as well as ATP binding cassette transporter (ABC) A1 mRNA with quantitative real time PCR analyses. As shown in Figure 3D, the mRNA levels of apoE were significantly elevated by TO treatment, indicating that LXRα activated with TO would have increased the transcription of apoE in S-Hep. ABCA1, which is regulated by LXR, was also upregulated by TO901317, although the levels of the induction were less than those observed with apoE (Figure 3E).

Distribution of apoE secreted from S-Hep among lipoproteins

As shown in the above experiments, we confirmed that the secretion of apoE was enhanced in S-Hep compared to M-Hep, and treatment of HepG2 cells with TO resulted in the augmentation of apoE secretion from HepG2 cells. We next analyzed the distributions of

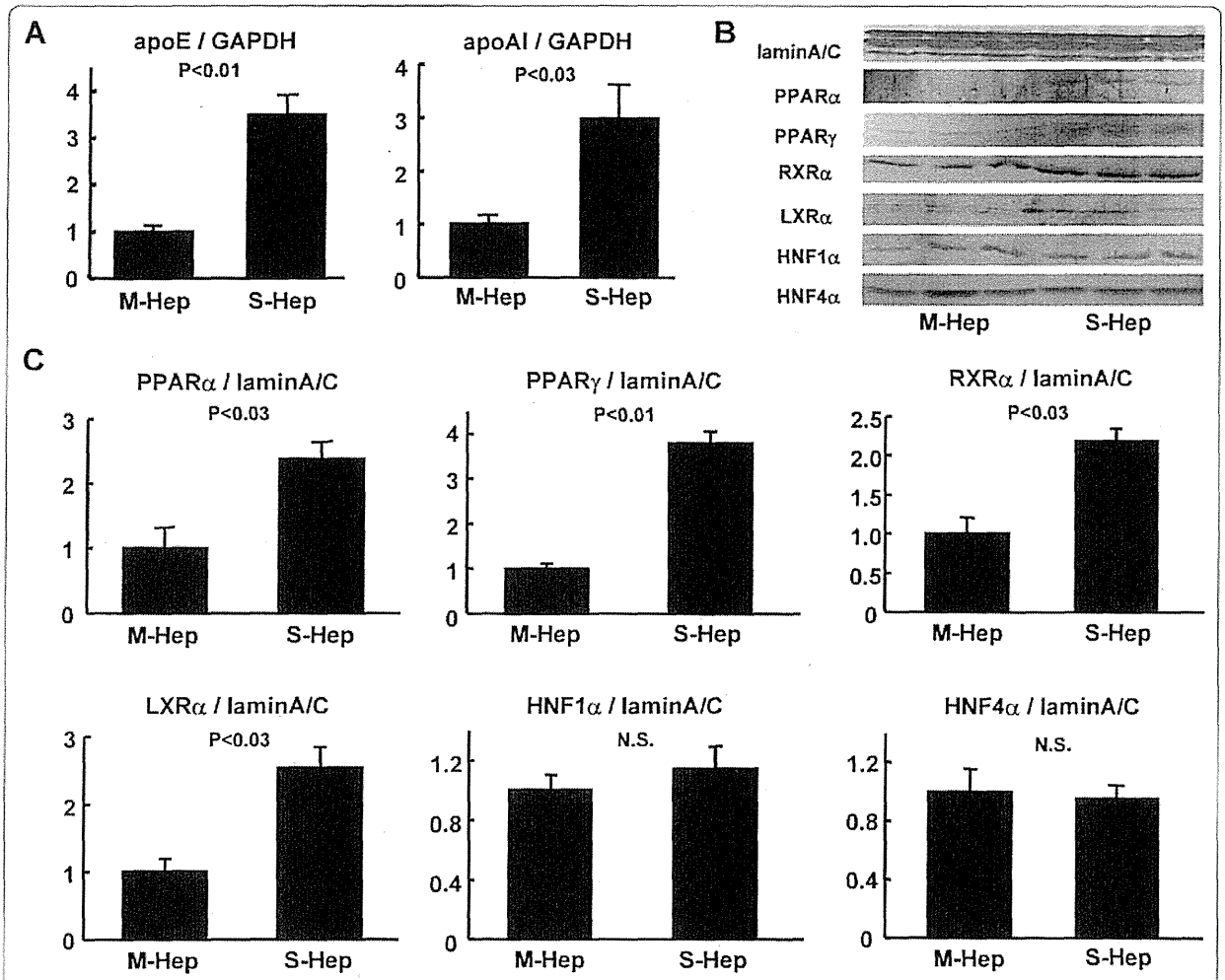

Figure 2 Differences in apolipoprotein mRNA and nuclear receptor protein levels among M-Hep and S-Hep. (A) Analyses of mRNA levels of apoE and apoA-I with quantitative RT-PCR (n = 4). GAPDH mRNA was used as the endogenous control for the expression levels of the gene of interest. (B, C) Western blot analyses were performed with the proteins prepared from nuclear fractions (Panel B), and nuclear protein levels were quantified with Image J utilizing lamin A/C as the internal control (Panel C) (n = 3). Y-axes in panels A and C represent ratios to the data of M-Hep.

apoE, together with those of apoB and apoA-I, among lipoproteins after fractionating the media with fast protein liquid chromatography (FPLC) which separated lipoproteins depending on their sizes. The results are shown in Figure 4 and 5: the fractions 21 - 26 corresponded to VLDL, fractions 29 - 37 to LDL, and fractions 38 - 48 to HDL based on the analysis of human plasma (data not shown). Both in S-Hep and M-Hep, apoA-I distribution was noted almost exclusively on fractions corresponding to HDL fractions, especially small HDL fractions; this distribution was not altered even with TO treatment. ApoB proteins were detected in fractions relevant to VLDL and LDL fractions, although the apoBs found in VLDL were scarce. In addition, no difference was observed in the distribution patterns of apoB between S-Hep and M-Hep, and treatment with TO did not alter these patterns. In contrast, unlike the findings of apoA-I and apoB, the distribution of apoE on lipoproteins was affected not only by the methods of the culture but also by the treatment with TO. ApoE secreted from M-Hep, regardless of the treatment with TO, were detected in the fractions spanning between those of LDL and HDL, suggesting its distribution on large HDL fractions; in addition, no apoE band was found in VLDL fractions even by the treatment with TO. On the other hand, the culture of HepG2 cells in spheroidal form rendered the apoE protein to reside on normal-sized HDL particles. Interestingly, treatment of S-Hep with TO not only increased the amount of secreted apoE incrementally with the increment of the

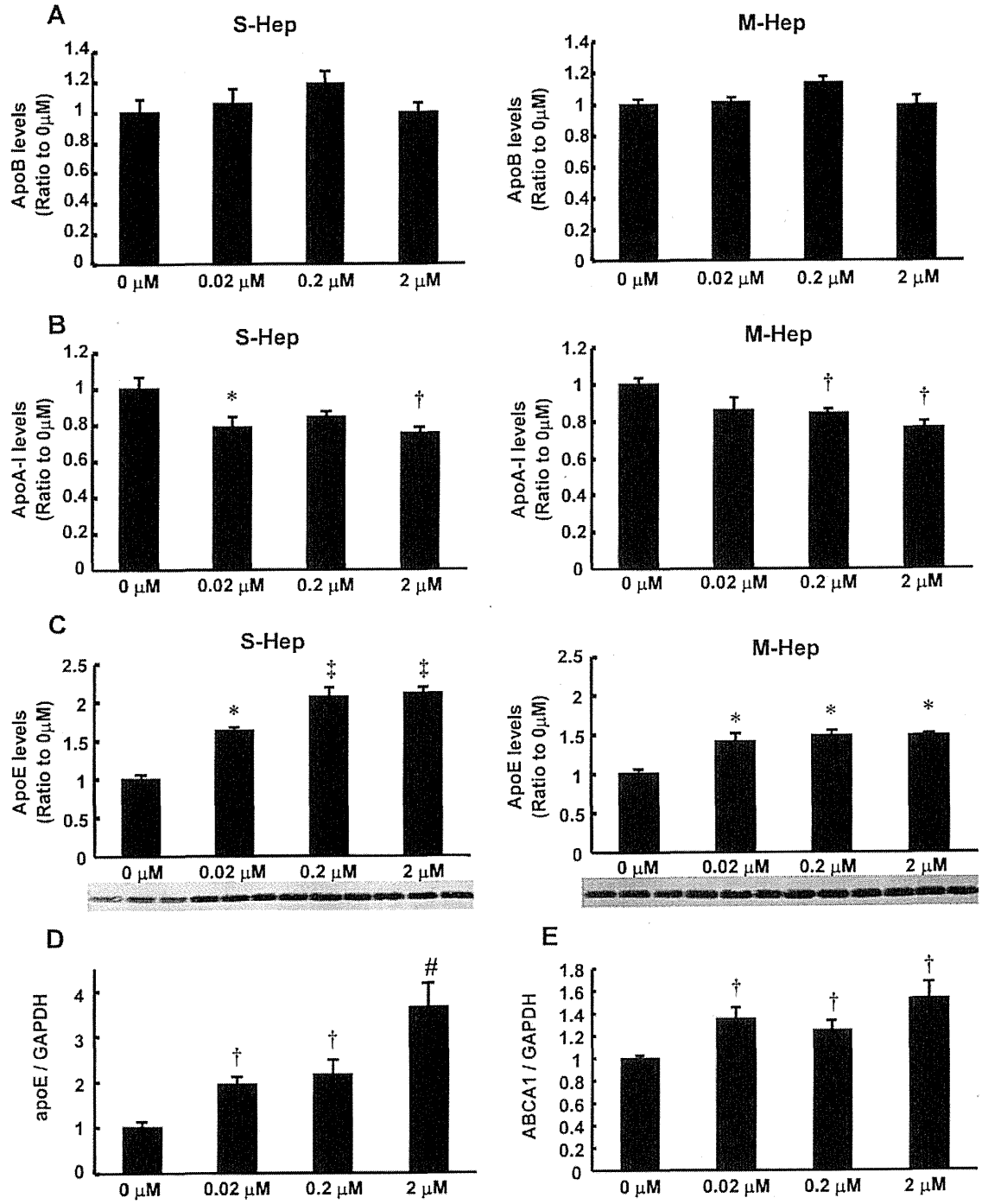

Figure 3 Effects of TO901317 treatment on the secretion and expression of apolipoproteins. (A-C) S-Hep and M-Hep were incubated with different concentration of TO901317, and the levels of apolipoproteins secreted in the medium were analyzed. Panel A, B and C represented apoB, apoA-I and apoE levels, respectively. (D, E) S-Hep were incubated with different concentration of TO901317, and mRNA levels of apoE (D) and ABCA1 (E) were analyzed. Data are mean ± SEM (n = 4). X-axes represent the concentration of TO901317. *: $P < 0.01$ compared with 0 μM, †: $P < 0.05$ with 0 μM, ‡: $P < 0.01$ with 0 and 0.02 μM, #: $P < 0.03$ with 0 and 0.02 μM.

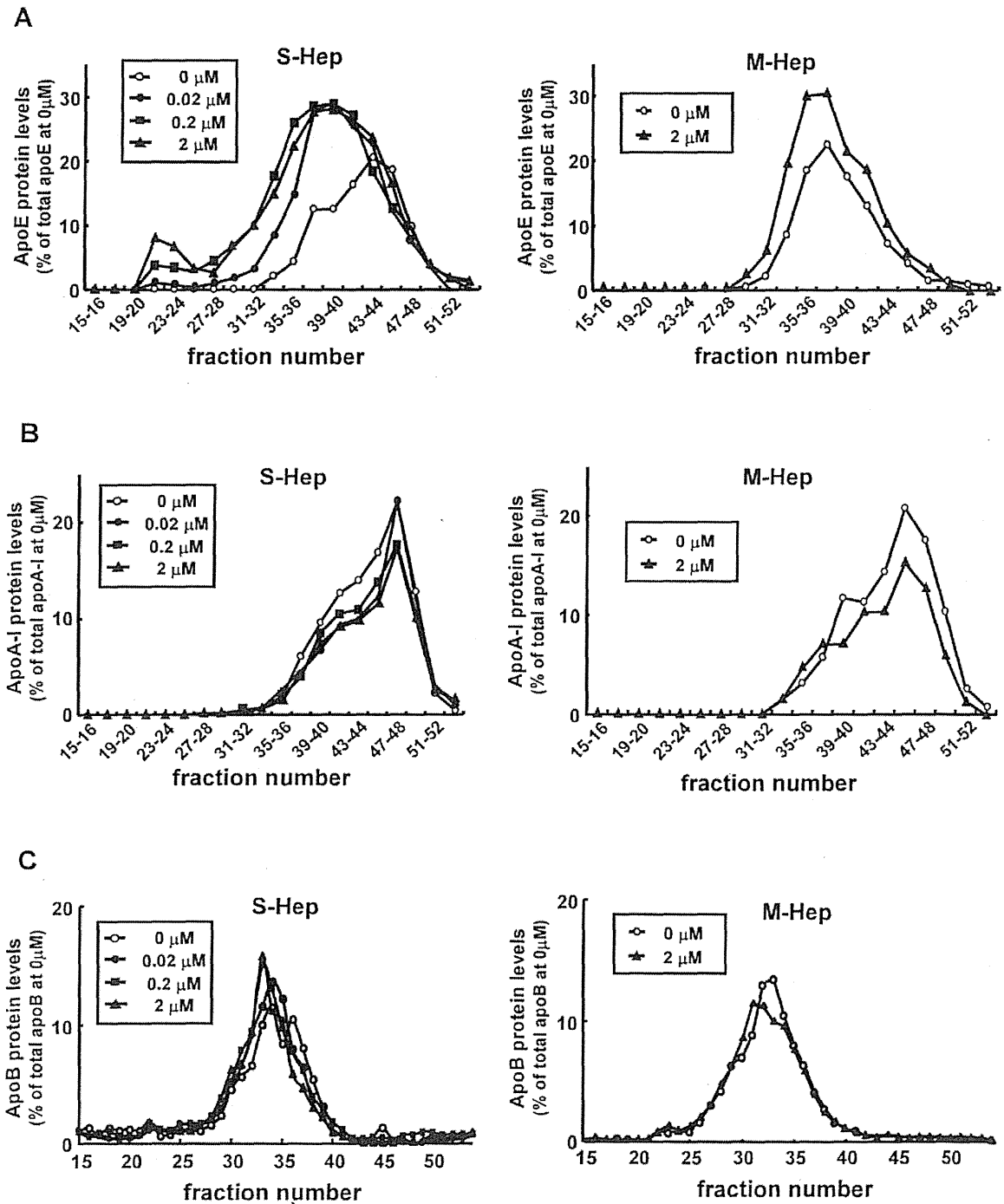

Figure 4 Effects of TO901317 treatment on the distribution of apolipoprotein among lipoproteins. Distribution of apoE (A), apoA-I (B), and apoB (C) on lipoprotein particles in the medium harvested from S-Hep (left) and M-Hep (right). Following the fractionation of the media with FPLC depending on the size of lipoproteins, fractionated samples were subjected to Western blot analyses or protein measurement with ELISA kits. White circles, black circles, squares and triangles represent the results from the medium of cells incubated with 0 μM, 0.02 μM, 0.2 μM and 2 μM of TO901317, respectively.

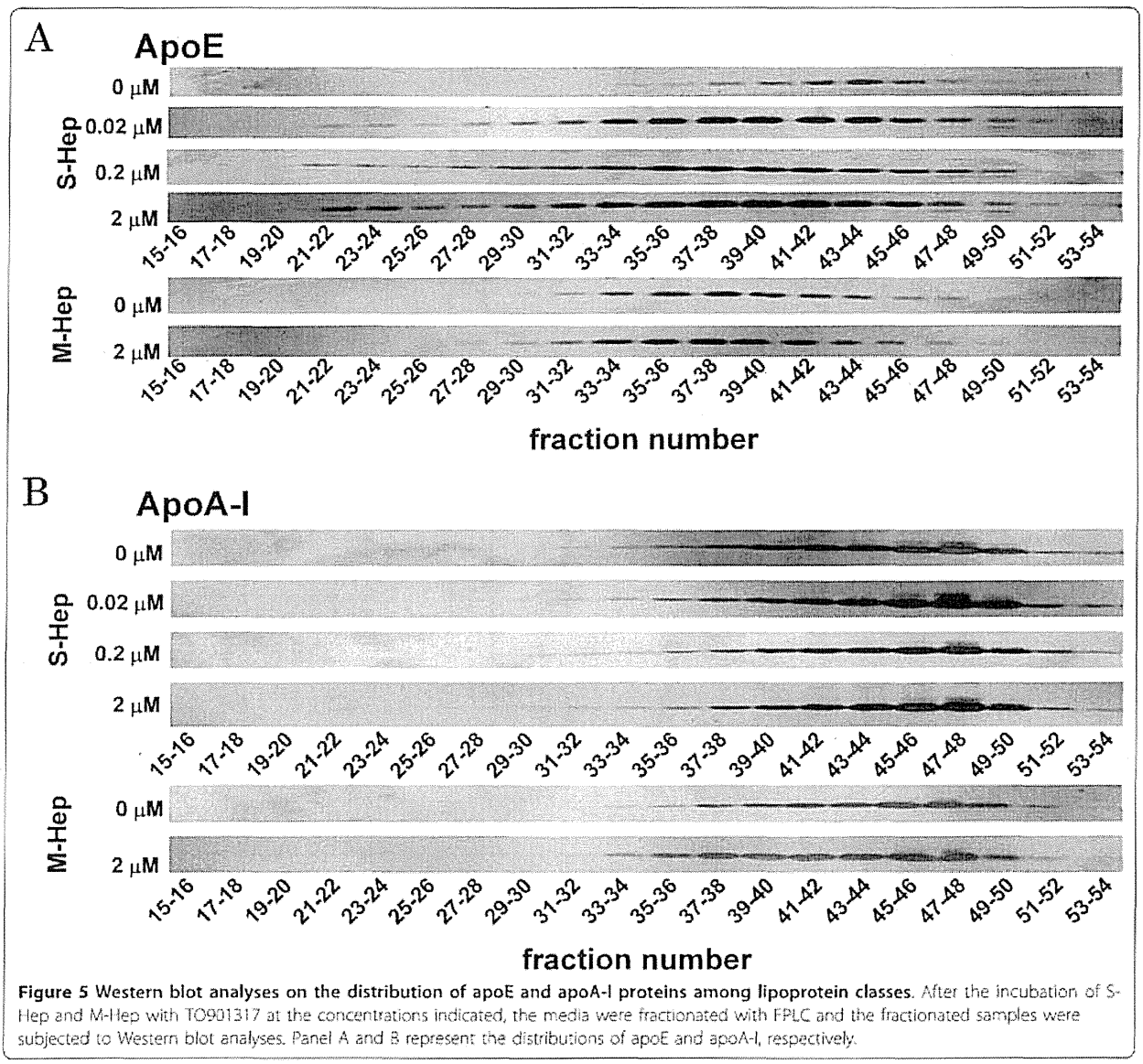

Figure 5 Western blot analyses on the distribution of apoE and apoA-I proteins among lipoprotein classes. After the incubation of S-Hep and M-Hep with TO901317 at the concentrations indicated, the media were fractionated with FPLC and the fractionated samples were subjected to Western blot analyses. Panel A and B represent the distributions of apoE and apoA-I, respectively.

dose of TO, but also rendered apoE to distribute on fractions larger than normal HDL. Based on the observation that neither apoA-I nor apoB was detected in these lipoprotein fractions, these fractions were assumed to be large apoE rich HDL. Furthermore, TO treatment of S-Hep resulted in the appearance of apoE on VLDL fractions; the amount of apoE on VLDL increased incrementally when the concentration of TO was increased up to 2 μM. In addition, as shown in Figure 6, treatment of S-Hep with 2 μM TO resulted in the increased triglycerides levels in the fractions where apoE protein increased with TO treatment. These results indicated that the TO treatment not merely resulted in the increased apoE protein levels in VLDL and large HDL fractions, but also resulted in the increased particle numbers and/or the enrichment of lipid content of VLDL and large HDL particles.

Discussion

Utilization of primary hepatocytes or hepatocyte-derived cell lines for in vitro experiments has helped us understand the lipid metabolism in the liver. However, it has been known that even the primary hepatocytes, when cultured in monolayer form, lose their differentiated, physiological functions quickly probably due to the loss of its three dimensional in vivo conformation in the experimental setting. In vivo experiments with rodents have also enabled us to elucidate the lipid metabolism

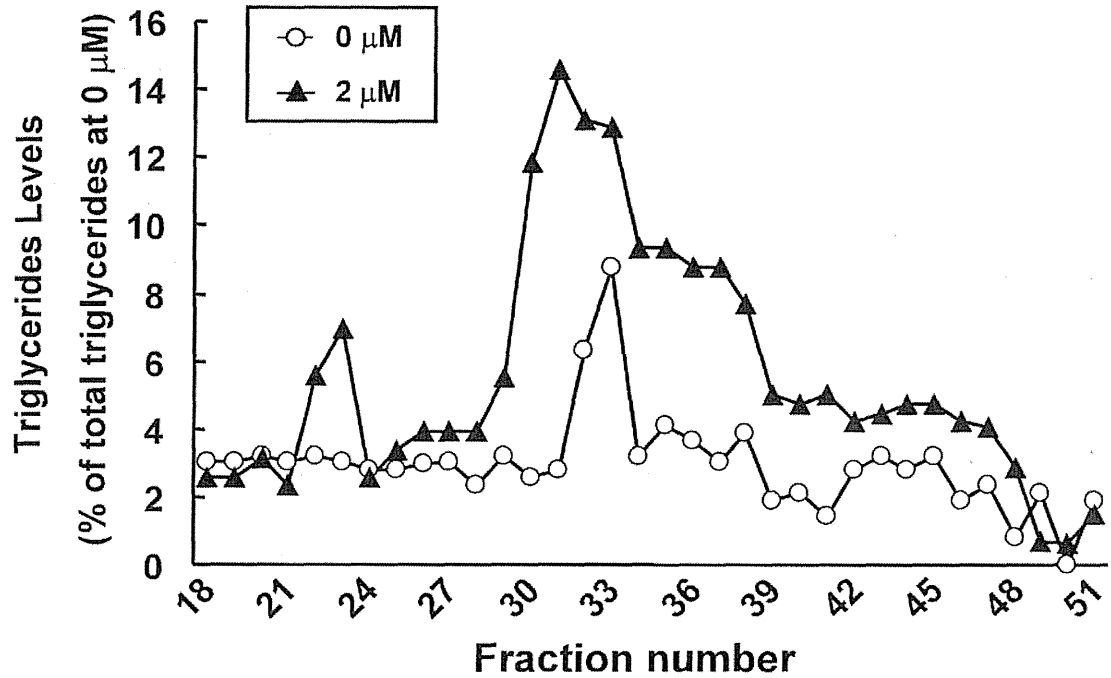

Figure 6 Analyses of triglyceride levels in the FPLC-fractionated samples. FPLC fractions obtained from S-Hep with or without 2 μM TO were subjected to the measurement of triglyceride (TG) levels with enzymatic method. White circles and triangles represent the results from the medium of cells incubated with 0 μM and 2 μM of TO901317, respectively.

in the liver; however, rodents might have been known to possess different properties from humans in lipid metabolism. Thus, in this study, in order to overcome these obstacles, we utilized 3-D spheroid culture system utilizing alginate beads, which has proven to be an easily-manipulative tactic to reproduce hepatocytes or hepatocytes-derived cells similar to their natural, differentiated in vivo counterparts.

Concordant with the previous observation by Khalil et al. [11], we were able to demonstrate that the culture of HepG2 cells in spheroid form resulted in enhanced albumin secretion compared to that in monolayer form, indicating that S-Hep utilized in this study had been more differentiated than M-Hep. The secretions of apoE, apoA-I, and apoB were also enhanced in S-Hep, and the nuclear protein contents of PPAR-α, PPAR-γ, LXR-α and RXR-α were increased in S-Hep, indicating that both of which are the features of differentiated hepatocytes or hepatocyte-derived cells. Furthermore, activation of LXR with TO901317 treatment of S-Hep resulted in the increased secretion of apoE protein which was accompanied by the up-regulation of apoE mRNA levels. Taking into account the previous study not showing a significant up-regulation of apoE gene with M-Hep treated with LXR activation [7], we assume that the differentiation of cells would be important to clearly examine the regulation of apoE gene in hepatocytes or hepatocyte-derived cells with LXR agonist, which is the case for macrophages and adipocytes [7].

The physiological regulation of apoE gene in the liver has so far not been clarified, although the baseline expression has been known to be controlled by distal hepatic enhancer elements [4,5] as well as the proximal promoter region to which TR4 orphan nuclear receptor binds [14]. Laffitte et al suggested that apoE enhancers and promoters containing LXRE would be important for the activation of apoE promoter in M-Hep; however, administration of LXR agonist in mice revealed a slight but non-significant role of LXR in the regulation of apoE in vivo [7]. Their observation does not depart at all from our present study, considering that murine lipid metabolism differs from that of humans in several respects. It is also plausible that factors other than LXR would regulate hepatic apoE gene in mice and probably in humans, considering that the degree of up-regulation of apoE gene observed in our study is less than those found in adipocytes and macrophages [7]. Further studies are needed to clarify these factors, and we believe that utilization of S-Hep would enable us to elucidate these factors.

In this study, we also found that the increased apoE secretion from S-Hep resulted in the alteration of

lipoprotein classes produced from the cells. One of the aspects of this alteration is the increased production of VLDL particles. In the state of hepatic steatosis, not only triglycerides but also cholesterol accumulate in hepatocytes [15], and the oxidative stress which increases in hepatic steatosis [16] transforms the cholesterol to oxysterol, which is a natural ligand for LXR. Because the production of apoE is one of the important determinants for the secretion of VLDL or VLDL-TG from the liver [3], the upregulation of apoE gene together with the increased production of triglycerides [17,18] by LXR activation facilitates the production of VLDL particles, resulting in the atherogenic lipid profile of the metabolic syndrome.

The other interesting finding in the alteration of lipoprotein production from S-Hep with TO901317 treatment was the increased production of large HDL particles containing apoE. Treatment with TO901317 prevented atherosclerosis in various mouse models [19-21], and increased apoE-rich HDL particles in C57BL6 mice [22,23]. These reagent effects have been attributed to the enhanced reverse cholesterol transport from macrophages [24] through the up-regulation of several key macrophagic proteins such as ABCA1 and apoE [25,26]. However, in this study, we did indicate that apoE-rich large HDL particles were also produced from the differentiated hepatocyte-derived cells, and that the induction was more pronounced with increasing increments of LXR activation. Although apoE-rich HDL has been speculated to play a role in delivering cholesterol to hormone-producing tissues such as adrenal tissues [27,28], several lines of study have indicated that apoE-rich HDL would also play an important role in reverse cholesterol transport; apoE-rich HDL is mainly contained in large HDL and large HDL has been demonstrated to extract cholesterol from macrophages [29]. It was also suggested that apoE-containing HDL efficiently enhanced cholesterol efflux [2,30]. Thus the increased production of apoE-rich large HDL particles from differentiated hepatocytes induced by LXR activation might have a role in the protection against atherosclerosis.

Conclusions

In summary, by utilizing the differentiated spheroid HepG2 cells, for the first time we were able to clearly demonstrate that LXR activation resulted in the up-regulation of human hepatic apoE, which also enhanced the production of VLDL particles and large apoE rich HDL particles. In future studies, investigation using HepG2 spheroids as surrogates to well-differentiated human hepatocytes would serve well as a model to precisely understand lipid metabolism in the liver.

Methods

Cell Culture and Experimental Protocol

HepG2 cells, purchased from American Type Culture Collection (ATCC, Manassas, VA), were cultured and maintained in DMEM (Sigma-Aldrich Co. St. Louis, MO) supplemented with 10% fetal bovine serum (FBS, Gibco BRL, Eggstein, Germany) and 1% penicillin/streptomycin (Gibco). For the experiment with M-Hep without TO (Sigma-Aldrich), 24 hours prior to the harvest of medium and cells, the medium was replaced with FBS-free medium to eliminate the plasma proteins derived from FBS in the medium. In the experimentation of M-Hep with TO, the medium was exchanged for that containing various concentrations of TO dissolved in DMSO at the cell confluency of around 70%. Two days later, the medium was replaced with the FBS-free medium containing the same concentration of TO, and cells were incubated for another 24 hours prior to the analysis. The collected cells were suspended in RIPA buffer (Santa Cruz Biotechnology, Santa Cruz, CA) for further analysis. The protein levels of the cell lysates were measured with Lowry methods (BioRad, Hercules, CA.) according to the manufacturer's protocol.

S-Hep were prepared following the methods described previously [11,12] with some modification. Briefly, HepG2 cells cultured in monolayer were detached completely with Trypsin-EDTA (Gibco) and suspended in α-MEM (Gibco) containing 10% FBS at the concentration of 0.5×10^6/mL. The medium containing HepG2 cells was mixed with the same amount of 2% alginate (Sigma). The mixed solution was dropped into 0.102 M $CaCl_2$/0.15 M NaCl (pH 7.4) solution at the speed of 1.5 ml/min through a 23 G cannula equipped inside another 19 G cannula from which the air was ejected at the speed of 1.2 L/min. This procedure yielded alginate-beads containing HepG2 cells, whose diameters ranged from 300 to 500 μm. The alginate beads were washed with DMEM twice and cultured in DMEM supplemented with 10% FBS and 1% penicillin/streptomycin. Prior to the harvest of cells and medium, beads containing S-Hep were washed twice with DMEM and cultured in FBS-containing DMEM with or without TO for two days. Thereafter, the medium was exchanged with FBS-free medium containing the same concentration of TO, and the cells were incubated for another 24 hours. Then the media were collected, and the cells were dissolved in RIPA buffer after releasing them from alginate beads with the incubation in PBS containing 4 mM EGTA (pH 7.4) for 10 minutes.

Quantification of Secreted Proteins in Medium

The concentrations of albumin, apoA-I and apoB in the media were measured by indirect sandwich enzyme-

linked immunosorbent assay (ELISA) with human albumin ELISA quantification kit (Bethyl laboratories, Inc. Montgomery, TX.) and ELISA kits for human apoA-I and apoB (Mabtech Inc. Nacka Strand, Sweden). For the quantification of apoE levels, the media, the volumes of which were adjusted according to cell protein levels, were subjected to 10% SDS-PAGE followed by Western-blot analysis with anti-apoE antibody (Chemicon International Inc, Temecula, CA), and the intensities of the bands were measured by Image J (from the NIH).

Preparation and Analysis of Nuclear Fraction

The nuclear fractions of HepG2 cells were obtained as follows: cells were dissolved in Buffer A (10 mM HEPES, 1.5 mM $MgCl_2$, 10 mM KCl, 0.5 mM DTT, 0.05% NP40, protease inhibitor cocktail (Roche, Mannheim, Germany), pH7.9) and incubated on ice for 10 minutes, centrifuged at 900 g for 10 minutes. The pellets were homogenized in Buffer B (5 mM HEPES. 1.5 mM $MgCl_2$, 0.2 M EDTA, 0.5 mM DTT, 26% glycerol, protease inhibitor cocktail, pH 7.9) supplemented with NaCl to the final concentration of 300 mM. Then, the solutions were centrifuged at 24,000 g for 20 minutes, and the supernatants were analyzed as the nuclear fractions of the cells. To quantify the levels of each nuclear protein, 30 μg of nuclear proteins extracted as above were subjected to 8% SDS-PGE followed by Western blot analyses with anti-Lamin A/C, anti-PPAR-α, anti-PPAR-γ, anti-RXR-α, anti-LXR-α, anti-HNF-1α, or anti-HNF-4α antibody (Santa Cruz Biotechnology).

Quantitative Real Time PCR

Total RNAs extracted from M-Hep and S-Hep with GenElute mammalian total RNA miniprep kit (Sigma-Aldrich) were subjected to reverse transcription with Superscript II enzyme (Invitrogen Co. Carlsbad, CA). Real-time quantitative PCR was performed with Light-Cycler system (Roche Diagnostics Basel, Switzerland). The expression levels of the gene of interest were normalized to those of the endogenous control GAPDH mRNA, and the amounts of target gene expressions were expressed as a ratio to those of control cells. The following primers were used: for GAPDH, forward 5' CCACTCCTCCACCTTTGA 3' and reverse 5' GTG GTCCAGGGGTCTTAC 3'; for apoA-I, forward 5' TGTCCCAGTTTGAAGGCT 3' and reverse 5' ATCC TTGCTCATCTCCTGC 3'; for apoE, forward 5' GGGT CGCTTTTGGGATTAC 3' and reverse 5' CAACT CCTTCATGGTCTCG 3'; for ABCA1, forward 5' AAATCCATTGTGGCTGC 3' and reverse 5' GGGA-GAGAGAGGTTGTGATAC 3'.

FPLC Analysis

The media of S-Hep or M-Hep, the total volumes of which were 12 mL, were concentrated to about 500 μl by centrifugation through Amicon Ultara-15 (Millipore Co., Bedford, MA). Then 200 μl of concentrated medium was separated by FPLC utilizing Superose 6 column. The levels of apoB in the separated fractions were analysed with ELISA method. For the analyses of apoE and apoA-I, the separated fractions were subjected to Western blots utilizing anti-apoE antibody and anti-apoA-I antibody (Chemicon). To raise the sensitivity of western blot analysis, after the incubation with primary antibodies, the membranes were incubated in biotin-conjugated anti-goat IgG antibody (Sigma) and then detected by Vecstatin ABC kit (Vector laboratories, Inc, Burlingame, CA). FPLC fractions obtained from S-Hep with or without 2 μM TO were subjected to the measurement of triglycerides (TG) levels with enzymatic method (WAKO Pure Chemical Industries, Osaka, Japan). To standardize the TG values among samples from with or without TO, the values obtained were adjusted utilizing the TG levels of the media which was corrected with cellular protein levels.

Statistical analysis

The results were expressed as mean ± SEM. Differences between two groups were evaluated with student's *t*-test, and the differences among more than assessed with one-way ANOVA, followed by multiple comparison tests. the *P* value less than 0.05 was deemed as statistically significant.

List of Abbreviations

apoA-I: apolipoprotein A-I; apoB: apolipoprotein B; apoE: apolipoprotein E; TO: TO901317; M-Hep: HepG2 cells cultured in monolayer; S-Hep: HepG2 cells cultured in spheroidal form; HNF: hepatocyte nuclear factor; LXR: liver × receptor; PPAR: peroxisome proliferator-activated receptor; RXR: retinoid × receptor; ABC: ATP-binding cassette transporter; FPLC: fast protein liquid chromatography; FBS: fetal bovine serum; ELISA: enzyme-linked immunosorbent assay.

Acknowledgements

This research was supported by Grant-In-Aid No. 20591079 (to KT) from the Japan Society for the Promotion of Science.

Author details

[1]Department of Metabolic Diseases, Graduate School of Medicine, The University of Tokyo, Tokyo 113-8655, Japan. [2]Department of Cardiovascular Medicine, Graduate School of Medicine, The University of Tokyo, Tokyo 113-8655, Japan. [3]Department of Infection Control and Prevention, Graduate School of Medicine, The University of Tokyo, Tokyo 113-8655, Japan. [4]Department of Gastroenterology, Graduate School of Medicine, The University of Tokyo, Tokyo 113-8655, Japan. [5]Department of Advanced Medical Science, The Institute of Medical Science, The University of Tokyo, Tokyo 108-8639, Japan. [6]Fourth Department of Internal Medicine, Mizonokuchi Hospital, Teikyo University School of Medicine, Kanagawa 213-8507, Japan. [7]Department of Metabolism, Diabetes and Nephrology, Preparatory Office for Aizu Medical Center, Fukushima Medical University, Fukushima 965-8555, Japan.

Authors' contributions
MK participated in study design, carried out experiments and data analysis, and drafted the initial manuscript. NaI and MH participated in several experiments. NOI participated in the real-time PCR study. KM and KK were involved in study design and drafting manuscript. KT conceived of the study, coordinated the study design and helped to draft the manuscript. All authors read and approved the final manuscript.

Competing interests
The authors declare that they have no competing interests.

Received: 8 July 2011 Accepted: 5 August 2011
Published: 5 August 2011

References

1. Zhang WY, Gaynor PM, Kruth HS: **Apolipoprotein E produced by human monocyte-derived macrophages mediates cholesterol efflux that occurs in the absence of added cholesterol acceptors.** *J Biol Chem* 1996, **271**:28641-6.
2. Hara M, Matsushima T, Satoh H, Iso-o N, Noto H, Togo M, Kimura S, Hashimoto Y, Tsukamoto K: **Isoform-dependent cholesterol efflux from macrophages by apolipoprotein E is modulated by cell surface proteoglycans.** *Arterioscler Thromb Vasc Biol* 2003, **23**:269-74.
3. Tsukamoto K, Maugeais C, Glick JM, Rader DJ: **Markedly increased secretion of VLDL triglycerides induced by gene transfer of apolipoprotein E isoforms in apoE-deficient mice.** *J Lipid Res* 2000, **41**:252-9.
4. Simonet WS, Bucay N, Lauer SJ, Taylor JM: **A far-downstream hepatocyte-specific control region directs expression of the linked human apolipoprotein E and C-I genes in transgenic mice.** *J Biol Chem* 1993, **268**:8221-9.
5. Allan CM, Taylor S, Taylor JM: **Two hepatic enhancers, HCR.1 and HCR.2, coordinate the liver expression of the entire human apolipoprotein E/C-I/C-IV/C-II gene cluster.** *J Biol Chem* 1997, **272**:29113-9.
6. Shih SJ, Allan C, Grehan S, Tse E, Moran C, Taylor JM: **Duplicated downstream enhancers control expression of the human apolipoprotein E gene in macrophages and adipose tissue.** *J Biol Chem* 2000, **275**:31567-72.
7. Laffitte BA, Repa JJ, Joseph SB, Wilpitz DC, Kast HR, Mangelsdorf DJ, Tontonoz P: **LXRs control lipid-inducible expression of the apolipoprotein E gene in macrophages and adipocytes.** *Proc Natl Acad Sci USA* 2001, **98**:507-12.
8. Driscoll DM, Mazzone T, Matsushima T, Getz GS: **Apoprotein E biosynthesis in the cholesterol-fed guinea pig.** *Arteriosclerosis* 1990, **10**:31-9.
9. Hennessy LK, Osada J, Ordovas JM, Nicolosi RJ, Stucchi AF, Brousseau ME, Schaefer EJ: **Effects of dietary fats and cholesterol on liver lipid content and hepatic apolipoprotein A-I, B, and E and LDL receptor mRNA levels in cebus monkeys.** *J Lipid Res* 1992, **33**:351-60.
10. Peet DJ, Turley SD, Ma W, Janowski BA, Lobaccaro JM, Hammer RE, Mangelsdorf DJ: **Cholesterol and bile acid metabolism are impaired in mice lacking the nuclear oxysterol receptor LXR alpha.** *Cell* 1998, **93**:693-704.
11. Khalil M, Shariat-Panahi A, Tootle R, Ryder T, McCloskey P, Roberts E, Hodgson H, Selden C: **Human hepatocyte cell lines proliferating as cohesive spheroid colonies in alginate markedly upregulate both synthetic and detoxificatory liver function.** *J Hepatol* 2001, **34**:68-77.
12. Damelin LH, Coward S, Choudhury SF, Chalmers SA, Cox IJ, Robertson NJ, Reval G, Miles M, Tootle R, Hodgson HJ, Selden C: **Altered mitochondrial function and cholesterol synthesis influences protein synthesis in extended HepG2 spheroid cultures.** *Arch Biochem Biophys* 2004, **432**:167-77.
13. Huuskonen J, Vishnu M, Chau P, Fielding PE, Fielding CJ: **Liver x receptor inhibits the synthesis and secretion of apolipoprotein A1 by human liver-derived cells.** *Biochemistry* 2006, **45**:15068-74.
14. Kim E, Yang Z, Liu NC, Chang C: **Induction of apolipoprotein E expression by TR4 orphan nuclear receptor via 5' proximal promoter region.** *Biochem Biophys Res Commun* 2005, **328**:85-90.
15. Cano A, Ciaffoni F, Safwat GM, Aspichueta P, Ochoa B, Bravo E, Botham KM: **Hepatic VLDL assembly is disturbed in a rat model of nonalcoholic fatty liver disease: is there a role for dietary coenzyme Q?** *J Appl Physiol* 2009, **107**:707-17.
16. Robertson G, Leclercq I, Farrell GC: **Nonalcoholic steatosis and steatohepatitis. II. Cytochrome P-450 enzymes and oxidative stress.** *Am J Physiol Gastrointest Liver Physiol* 2001, **281**:G1135-9.
17. Chisholm JW, Hong J, Mills SA, Lawn RM: **The LXR ligand T0901317 induces severe lipogenesis in the db/db diabetic mouse.** *J Lipid Res* 2003, **44**:2039-48.
18. Grefhorst A, Elzinga BM, Voshol PJ, Plosch T, Kok T, Bloks VW, van der Sluijs FH, Havekes LM, Romijn JA, Verkade HJ, Kuipers F: **Stimulation of lipogenesis by pharmacological activation of the liver x receptor leads to production of large, triglyceride-rich very low density lipoprotein particles.** *J Biol Chem* 2002, **277**:34182-90.
19. Verschuren L, de Vries-van der Weij J, Zadelaar S, Kleemann R, Kooistra T: **LXR agonist suppresses atherosclerotic lesion growth and promotes lesion regression in apoE*3Leiden mice: time course and mechanisms.** *J Lipid Res* 2009, **50**:301-11.
20. Peng D, Hiipakka RA, Dai Q, Guo J, Reardon CA, Getz GS, Liao S: **Antiatherosclerotic effects of a novel synthetic tissue-selective steroidal liver x receptor agonist in low-density lipoprotein receptor-deficient mice.** *J Pharmacol Exp Ther* 2008, **327**:332-42.
21. Terasaka N, Hiroshima A, Koieyama T, Ubukata N, Morikawa Y, Nakai D, Inaba T: **T-0901317, a synthetic liver x receptor ligand, inhibits development of atherosclerosis in LDL receptor-deficient mice.** *FEBS Lett* 2003, **536**:6-11.
22. Jiang XC, Beyer TP, Li Z, Liu J, Quan W, Schmidt RJ, Zhang Y, Bensch WR, Eacho PI, Cao G: **Enlargement of high density lipoprotein in mice via liver x receptor activation requires apolipoprotein E and is abolished by cholesteryl ester transfer protein expression.** *J Biol Chem* 2003, **278**:49072-8.
23. Cao G, Beyer TP, Yang XP, Schmidt RJ, Zhang Y, Bensch WR, Kauffman RF, Gao H, Ryan TP, Liang Y, Eacho PI, Jiang XC: **Phospholipid transfer protein is regulated by liver x receptors in vivo.** *J Biol Chem* 2002, **277**:39561-5.
24. Zanotti I, Poti F, Pedrelli M, Favari E, Moleri E, Franceschini G, Calabresi L, Bernini F: **The LXR agonist T0901317 promotes the reverse cholesterol transport from macrophages by increasing plasma efflux potential.** *J Lipid Res* 2008, **49**:954-60.
25. Beyea MM, Heslop CL, Sawyez CG, Edwards JY, Markle JG, Hegele RA, Huff MW: **Selective up-regulation of LXR-regulated genes ABCA1, ABCG1, and APOE in macrophages through increased endogenous synthesis of 24(S),25-epoxycholesterol.** *J Biol Chem* 2007, **282**:5207-16.
26. Levin N, Bischoff ED, Daige CL, Thomas D, Vu CT, Heyman RA, Tangirala RK, Schulman IG: **Macrophage liver x receptor is required for antiatherogenic activity of LXR agonists.** *Arterioscler Thromb Vasc Biol* 2005, **25**:135-42.
27. Hammami M, Meunier S, Maume G, Gambert P, Maume BF: **Effect of rat plasma high density lipoprotein with or without apolipoprotein E on the cholesterol uptake and on the induction of the corticosteroid biosynthetic pathway in newborn rat adrenocortical cell cultures.** *Biochim Biophys Acta* 1991, **1094**:153-60.
28. Kraemer FB: **Adrenal cholesterol utilization.** *Mol Cell Endocrinol* 2007, **265-266**:42-5.
29. Matsuura F, Wang N, Chen W, Jiang XC, Tall AR: **HDL from CETP-deficient subjects shows enhanced ability to promote cholesterol efflux from macrophages in an apoE- and ABCG1-dependent pathway.** *J Clin Invest* 2006, **116**:1435-42.
30. Krimbou L, Marcil M, Chiba H, Genest J Jr: **Structural and functional properties of human plasma high density-sized lipoprotein containing only apoE particles.** *J Lipid Res* 2003, **44**:884-92.

doi:10.1186/1476-511X-10-134
Cite this article as: Kurano *et al.*: LXR agonist increases apoE secretion from HepG2 spheroid, together with an increased production of VLDL and apoE-rich large HDL. *Lipids in Health and Disease* 2011 10:134.

Clin Chem Lab Med 2011;49(4):751–752 © 2011 by Walter de Gruyter • Berlin • New York. DOI 10.1515/CCLM.2011.103

Letter to the Editor

Evaluation of multiplex PCR using dual-priming oligonucleotide for the detection of *vanA* and *vanB* in vancomycin-resistant enterococci

Ran Nagai[1,2], Ryoichi Saito[2,*], Saho Koyano[1,2], Noboru Okamura[2], Hiromitsu Yokota[3], Takatoshi Kitazawa[1] and Kyoji Moriya[1]

[1] Department of Infection Control and Prevention, The University of Tokyo Hospital, Tokyo, Japan
[2] Microbiology and Immunology, Department of Moleculo-Genetic Sciences, Graduate School of Health Care Sciences, Tokyo Medical and Dental University, Tokyo, Japan
[3] Department of Clinical Laboratory, The University of Tokyo Hospital, Tokyo, Japan

Keywords: dual-priming oligonucleotide; multiplex PCR; *vanA*; *vanB*.

Vancomycin-resistant enterococci (VRE) are multi-drug resistant pathogens that may cause serious nosocomial infections. Among the vancomycin resistance (Van) genes, *vanA* and *vanB* remain the most clinically relevant as they are associated with transposons and may mediate horizontal transfer of vancomycin resistance to other bacteria (1). Therefore, early detection of VRE is crucial for the management and treatment of both colonized and infected patients, and for appropriate implementation of infection control measures to prevent the spread of VRE. Until now, since PCR methods for detecting and identifying VRE are not cost-effective, a number of studies have attempted to develop and evaluate multiplex PCR for screening for VRE (2, 3). Generally, the results have shown that multiplex PCR is quicker and has higher sensitivity compared with conventional culture for the detection of *vanA* and *vanB*.

Recently, the Seeplex VRE detection assay (S-VRE; Seegene Inc., Seoul, Korea), based on a multiplex PCR using a dual-priming oligonucleotide (DPO) system, has been introduced. The DPO system is a new molecular technique for PCR, which contains two separate priming regions joined by a polydeoxyinosine linker. These primers allow a wide range of annealing temperatures and provide high sensitivity and specificity which helps prevent false-positive results (4–6). In this study, we evaluated the performance of S-VRE for the simultaneous detection of *vanA* and *vanB* in VRE.

Five VRE strains [three *Enterococcus faecium* isolated in a clinical laboratory (*vanA*), one *Enterococcus faecalis* ATCC51299 (*vanB*) and one *Enterococcus casseliflavus* isolated in a clinical laboratory (*vanC-2*)] and *E. faecalis* ATCC 29212 were used as glycopeptide resistant controls and a wild type control, respectively. To determine the analytical sensitivity of the S-VRE, DNA templates were obtained from the supernatant of boiled extracts of a clinical isolate of *E. faecium* carrying *vanA* and *E. faecalis* V583 carrying *vanB* harvested from a trypticase soy agar plate with 5% defibrinated sheep blood (Nissui Pharmaceutical, Tokyo, Japan). Their concentrations were measured using a spectrophotometer (Thermo Fisher Scientific, Wilmington, DE, USA). The number of genomic copies for S-VRE was calculated by assuming the molecular size of *E. faecalis* V583 to be 3.21 Mbp (GenBank accession no. NC_004668). The amplification profile of this assay is as follows: initial denaturation at 94°C for 15 min, 35 cycles of amplification (denaturation at 94°C for 30 s, annealing at 60°C for 1 min, and extension at 72°C at 1 min), and final extension at 72°C for 10 min. Amplification was performed using a thermal cycler (Applied Biosystems, Foster City, CA, USA). Also, multiplex PCR amplification of *vanA* and *vanB* was performed using primer sets according to a method described previously [K-PCR; 3]. Amplified PCR products were separated by electrophoresis in 2.0% agarose and visualized by ethidium bromide staining. Each assay was performed three times to check for variation. For clinical evaluation, a total of 50 stool specimens collected from hospitalized patients between May and June 2009 were included in this study and analyzed in singlicate. Stool specimens for culture were directly inoculated onto VRE agar plates (Becton Dickinson, Tokyo, Japan) containing 6 mg/L vancomycin. All isolates growing on VRE agar plates were regarded as presumptive VRE and identified using the VITEK Legacy system (Sysmex-bioMerieux, Tokyo, Japan).

The minimum concentrations of *vanA* and *vanB* detected by S-VRE were 2.5 and 8.5×10^2 copies/reaction, respectively (Figure 1). Similarly, those detected by K-PCR were 2.5×10^3 and 8.5×10^3 copies/reaction, respectively. Compared to K-PCR, S-VRE of *vanA* and *vanB* had 1.0×10^3

*Corresponding author: Ryoichi Saito, PhD, Microbiology and Immunology, Department of Moleculo-Genetic Sciences, Graduate School of Health Care Sciences, Tokyo Medical and Dental University, 1-5-45 Yushima, Bunkyo-ku, Tokyo 113-8510, Japan
Phone/Fax: +81-3-5803-5375, E-mail: saito-lab@umin.ac.jp
Previously published online January 31, 2011

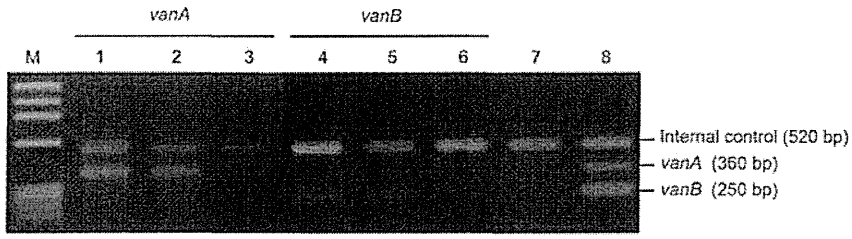

Figure 1 Analytical sensitivity of the Seeplex VRE detection assay for the detection of *vanA* and *vanB* in enterococcal isolates using serial dilutions of the DNA template.
Lane M, φ×174/*Hae*III; lanes 1, 2, 3, 4, 5, and 6, 2.5×10^1, 2.5, 0.25, 8.5×10^3, 8.5×10^2 and 8.5×10^1 copies/reaction, respectively; lane 7, the template DNA of a glycopeptide-susceptible *E. faecalis*; lane 8, VRE size marker.

and 10-fold higher sensitivity, respectively. For clinical evaluation, none of the isolates growing on VRE agar plates was positive for *vanA* and/or *vanB* by S-VRE and K-PCR. However, the sensitivity of S-VRE applied to stool specimens with varying densities of *vanA*- or *vanB*-positive isolates was 10^3 cfu/g stool (*vanA*) and 10^4 cfu/g stool (*vanB*).

In this study, S-VRE was considerably more sensitive and easy to perform compared with K-PCR for detecting the Van genes. Furthermore, S-VRE can check the presence of PCR inhibitors since it contains an internal control. These results were similar to previous findings that DPO-based multiplex PCR was a useful diagnostic method (4–6). Moreover, D'Agata et al. (7) demonstrated that the mean density of VRE was 6 ± 2 $\log_{10}$ cfu/g stool in patients with VRE colonization or infection. Therefore, we have demonstrated that S-VRE offers detection of VRE directly from colonies growing on VRE agar plates within a few hours, with high sensitivity, and can help with the rapid deployment of infection control and prevention measures.

One limitation of this study is the small number of VRE isolates. However, our study indicates that S-VRE represents a significant improvement over the previous method of multiplex PCR for detection of *vanA* and *vanB*.

Conflict of interest statement

Authors' conflict of interest disclosure: The authors stated that there are no conflicts of interest regarding the publication of this article.

Research funding: None declared.
Employment or leadership: None declared.
Honorarium: None declared.

References

1. Gold HS. Vancomycin resistant enterococci: mechanism and clinical observations. Clin Infect Dis 2001;33:210–21.
2. Patel R, Uhl JR, Kohner P, Hopkins MK, Cockerill FR 3rd. Multiplex PCR detection of vanA, vanB, vanC-1, and vanC-2/3 genes in enterococci. J Clin Microbiol 1997;35:703–7.
3. Kariyama R, Mitsuhata R, Chow JW, Clewell DB, Kumon H. Simple and reliable multiplex PCR assay for surveillance isolates of vancomycin-resistant enterococci. J Clin Microbiol 2000;38:3092–5.
4. Chun JY, Kim KJ, Hwang IT, Kim YJ, Lee DH, Lee IK, et al. Dual priming oligonucleotide system for the multiplex detection of respiratory viruses and SNP genotyping of CYP2C19 gene. Nucleic Acids Res 2007;35:e40.
5. Horii T, Ohtsuka H, Osaki M, Ohkuni H. Use of a dual priming oligonucleotide system to detect multiple sexually transmitted pathogens in clinical specimens. Lett Appl Microbiol 2009;49:46–52.
6. Drews SJ, Eshaghi A, Pyskir D, Chedore P, Lombos E, Broukhanski G, et al. The relative test performance characteristics of two commercial assays for the detection of Mycobacterium tuberculosis complex in paraffin-fixed human biopsy specimens. Diagn Pathol 2008;3:37.
7. D'Agata EM, Gautam S, Green WK, Tang YW. High rate of false-negative results of the rectal swab culture method in detection of gastrointestinal colonization with vancomycin-resistant enterococci. Clin Infect Dis 2002;34:167–72.

Journal of Chromatography A, 1218 (2011) 3447–3452

Contents lists available at ScienceDirect

Journal of Chromatography A

journal homepage: www.elsevier.com/locate/chroma

Liquid chromatographic separation of proteins derivatized with a fluorogenic reagent at cysteinyl residues on a non-porous column for differential proteomics analysis

Akiyo Koshiyama [a], Tomoko Ichibangase [a], Kyoji Moriya [b], Kazuhiko Koike [c], Itaru Yazawa [d], Kazuhiro Imai [a,*]

[a] Research Institute of Pharmaceutical Sciences, Musashino University, 1-1-20 Shinmachi, Nishitokyo-shi, Tokyo 202-8585, Japan
[b] Department of Infection Control and Prevention, Graduate School of Medicine, University of Tokyo, 7-3-1 Hongo, Bunkyo-ku, Tokyo 113-8655, Japan
[c] Department of Internal Medicine, Graduate School of Medicine, University of Tokyo, 7-3-1 Hongo, Bunkyo-ku, Tokyo 113-8655, Japan
[d] Imtakt Corporation, Kyoto Research Park, Chudoji Minami, Shimogyo-ku, Kyoto 600-8813, Japan

ARTICLE INFO

Article history:
Received 1 February 2011
Received in revised form 24 March 2011
Accepted 26 March 2011
Available online 4 April 2011

Keywords:
FD-LC-MS/MS method
Non-porous column
Wide-pore column
Differential proteomics analysis
Hepatocarcinogenesis

ABSTRACT

A wide-pore (30 nm) reversed-phase column (Intrada WP-RP, particle size 3 μm) was recently utilized for protein separation in differential proteomics analysis with fluorogenic derivatization-liquid chromatography–tandem mass spectrometry (FD-LC-MS/MS), and exerted a tremendous effect on finding biomarkers (e.g., for breast cancer). Further high-performance separation is required for highly complex protein mixtures. A recently prepared non-porous small-particle reversed-phase column (Presto FF-C18, particle size: 2 μm) was expected to more effectively separate derivatized protein mixtures than the wide-pore column. A preliminary experiment demonstrated that the peak capacity of the former was threefold greater than that of the latter in gradient elution of a fluorogenic derivatized model peptide, calcitonin. The FD-LC-MS/MS method with a non-porous column was then optimized and applied to separate liver mitochondrial proteins that were not efficiently separated with the wide-pore column. As a result, high-performance separation of mitochondrial proteins was accomplished, and differential proteomics analysis of liver mitochondrial proteins in a hepatitis-infected mouse model was achieved using the FD-LC-MS/MS method with the non-porous column. This result suggests the non-porous small-particle column as a replacement for the wide-pore column for differential proteomics analysis in the FD-LC-MS/MS method.

1. Introduction

High-performance liquid chromatography (HPLC) has been used for separating highly complex mixtures of compounds, such as cell and tissue extracts. However, because efficient separation of intact proteins is difficult, one-dimensional (1D) or multidimensional (mD) HPLC is usually performed with peptides generated by digesting intact proteins in proteomics analysis (reviewed in Ref. [1]). In contrast, we have developed the first reproducible quantification method using 1D HPLC for proteomics analysis, called fluorogenic derivatization-liquid chromatography-tandem mass spectrometry (FD-LC-MS/MS) with a database-searching algorithm. Intact protein mixtures were first derivatized at cysteinyl residues with a fluorogenic reagent, followed by isolation with a wide-pore reversed-phase column, Intrada WP-RP (30 nm pore size and 3 μm particle) (Imtakt, Kyoto, Japan), digestion of the derivatized proteins, and identification of the isolated proteins [2]. Application to real biological samples indicated the appearance of more than 400 or 500 proteins on a chromatogram [3–7]. Differential proteomics analysis demonstrated the existence of many proteins related to an early stage of Parkinson's disease [3], developmental stages of hepatocarcinogenesis [4], metastatic or normal breast cancer cells [5], the aging of rat brain regions [6], and the running speed of horses [7].

Differential proteomics analysis of liver proteins between hepatitis C virus (HCV) core gene transgenic (Tg) and non-transgenic (NTg) mice indicated some disease-related proteins in the developmental stages of hepatocarcinogenesis [4]. Since many of those proteins were related to the function of mitochondrial events (e.g., respiration, electron-transfer system, and β-oxidation), we further performed differential proteomics analysis of liver mitochondrial proteins between Tg and NTg mice by FD-LC-MS/MS to clarify the role of mitochondrial proteins. In a preliminary experiment, however, it was difficult to separate the mitochondrial protein mixture

* Corresponding author. Tel.: +81 42 468 9787; fax: +81 42 468 9787.
E-mail address: k-imai@musashino-u.ac.jp (K. Imai).

0021-9673/$ – see front matter © 2011 Elsevier B.V. All rights reserved.
doi:10.1016/j.chroma.2011.03.070

effectively using the conventional wide-pore column that was used for the FD–LC–MS/MS method. Therefore, we searched for other columns that have higher-performance separation ability than the wide-pore column.

According to recent technical developments, the use of a stationary phase of small and non-porous particles (sub-2 μm) reduces eddy diffusion and mass-transfer resistance in the mobile phase more than porous particles [8]. Chong et al. used sub-2 μm non-porous particles for separating intact proteins in biological samples [9]. However, the reproducibility of the retention time of each protein was very low, probably due to the hydrophobicity of the intact proteins and the large amount of proteins provided for ultraviolet detection, which could prevent using a non-porous column for differential proteomics analysis. In contrast, with FD–LC–MS/MS, the non-porous column seems to be useful because the proteins are derivatized into less hydrophobic ones with the hydrophilic reagent, and one or two orders of magnitude less amount of proteins is sufficient for fluorescence detection than for ultraviolet detection.

Therefore, in this study, we applied a non-porous small-particle reversed-phase column (Presto FF-C18, 2 μm particle, Imtakt) to the FD–LC–MS/MS method. Based on an investigation of column lengths and flow rates for the non-porous column, the optimized FD–LC–MS/MS method was applied to liver mitochondrial proteomics analysis, resulting in high-performance separation of the mitochondrial proteins. This result suggested the non-porous small-particle column as a replacement for the wide-pore column in differential proteomics analysis utilizing the FD–LC–MS/MS method. Also, the result of liver mitochondrial proteomics analysis indicated proteins related to hepatocarcinogenesis; thus, the roles of proteins in hepatocarcinogenesis will be investigated.

2. Experimental

2.1. Reagents

For this study, 7-chloro-N-[2-(dimethylamino)ethyl]-2,1,3-benzoxadiazole-4-sulfonamide (DAABD-Cl) and Buffer Solution pH 8.7 (6 M Guanidine Hydrochloride) were obtained from Tokyo Chemical Industry (Tokyo, Japan). In addition, 3-[(3-cholamidopropyl)dimethylammonio]propanesulfonate (CHAPS) and ethylenediamine-N,N,N′,N′-tetraacetic acid disodium salt (Na_2EDTA) were obtained from Dojindo Laboratories (Kumamoto, Japan). Tris(2-carboxyethyl)phosphine hydrochloride (TCEP) and β-lactoglobulin (M.W. 18,363) were purchased from Sigma–Aldrich (St. Louis, MO, USA). Calcitonin (M.W. 3,418) was purchased from Peptide Institute (Osaka, Japan). Trifluoroacetic acid (TFA) was obtained from Wako Pure Chemical Industries (Osaka, Japan). Acetonitrile (HPLC grade) was obtained from Kanto Chemical (Tokyo, Japan). All the other reagents were of analytical reagent grade and were used without further purification. Water was used after purification with the Milli-Q system (Nihon Millipore, Tokyo, Japan).

2.2. Columns

Non-porous spherical silica (2 μm particle and 2 m^2/g specific surface area) was utilized as packing material in the Presto FF-C18 column (Fig. 1) (Imtakt, Kyoto, Japan). Octadecylsilane (ODS) binds to functional groups on packing materials, indicating that Presto FF-C18 is useful for reversed-phase separation in HPLC. However, wide-pore spherical silica (30 nm pore size, 3 μm particle, and 100 m^2/g specific surface area) was utilized in the Intrada WP-RP column (Imtakt). Reversed-phase ligands exist on the surface of the packing materials of Intrada WP-RP, which was used as a conventional protein separation column for the FD–LC–MS/MS method. Presto FF-C18 columns were adopted with 4.6 mm i.d. and 50–250 mm length, while Intrada WP-RP with 4.6 mm i.d. and 250 mm length was usually utilized for protein separation [2–7].

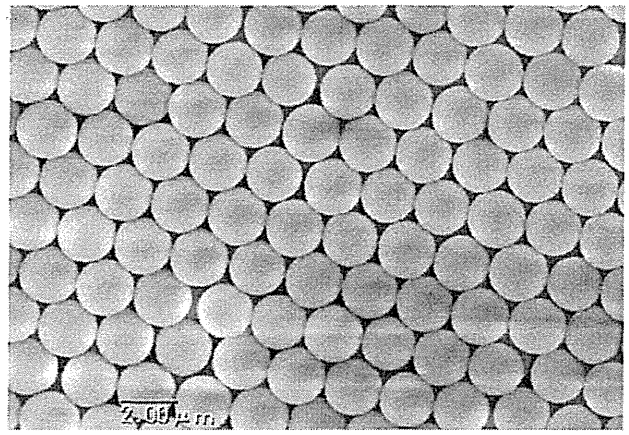

Fig. 1. Electron microscopic image of non-porous spherical silica (2 μm particle) utilized as a packing material in a Presto FF-C18 column.

2.3. FD reaction and separation of DAABD-calcitonin on the non-porous or the wide-pore column

A 10 μL aliquot of 5 μM calcitonin (Peptide Institute, Osaka, Japan) was mixed with 60 μL of 16.7 mM CHAPS/3.33 mM Na_2EDTA/0.833 mM TCEP in 6 M guanidine buffer (pH 8.7), 25 μL of 6 M guanidine buffer (pH 8.7), and 5.0 μL of 140 mM DAABD-Cl in acetonitrile. Each reaction mixture was incubated at 40 °C for 10 min, and the reaction was stopped with 3.0 μL of 20% TFAaq. The reaction mixture was then diluted threefold with the mobile phase. A 10 μL aliquot of the diluted reaction mixture was injected into an HPLC system that consisted of a pump (L-2100, Hitachi) and a fluorescence detector (L-2485, Hitachi). Fluorescence detection was carried out at 505 nm (excitation at 395 nm). Separation was performed on the non-porous column (4.6 i.d. × 50, 100, 150, or 250 mm) or the wide-pore column (4.6 i.d. × 250 mm) (Imtakt, Kyoto, Japan). The column temperature was set at 60 °C, and the flow rate was 0.2–0.5 mL/min. The gradient elution was 10–40% B over 60 min ((A) water:acetonitrile:TFA = 90:10:0.10, v/v/v; (B) water:acetonitrile:TFA = 30:70:0.20, v/v/v).

2.4. Preparation of liver mitochondrial sample and determination of total proteins

Sixteen-month-old Tg and NTg mice were used for analysis. Progression of disease state and morphological features were described in previous reports [4,10].

A preliminary study clearly indicated that an extraction procedure utilizing a mitochondrial isolation commercial kit was not useful, due to the low repeatability in isolation handling. Therefore, in this study, mitochondria were extracted from liver samples (100 mg) by density-gradient centrifugation using a mannitol/sucrose solution, as reported by Lopez et al. [11]. The mitochondrial pellet obtained was suspended with twice-volume of 2% CHAPS in 6 M guanidine buffer (pH 8.7). The suspension was sonicated for 15 s on ice four times at 15 s intervals. The sonicated suspension was centrifuged at 13,000 g for 2 min at 4 °C. The supernatant was then collected and stored as a soluble fraction at −80 °C after freezing with liquid nitrogen. The total liver mitochondrial proteins were determined with a BCA™ Protein Assay

Kit (Thermo Scientific, Rockford, IL, USA), following the written instructions. Bovine serum albumin was used as a protein standard.

2.5. FD–LC–MS/MS method for liver mitochondrial proteomics analysis

The previous method was used for the FD procedure for liver mitochondrial proteins with DAABD-Cl [4], except for the amount of total protein; in brief, 60 μg of liver mitochondrial proteins was derivatized in 100 μL reaction mixture. Twenty microliters of the reaction mixture (12 μg proteins) was subjected to HPLC. Sample proteins amount per injection was low enough as compared to the maximum (24 μg) for separation on the non-porous column. The overall system consisted of a Hitachi L-2000 series HPLC system with a non-porous column (4.6 i.d. × 250 mm) at a column temperature of 60 °C [2] and a flow rate of 0.3 mL/min. Fluorescence detection was carried out at 505 nm (excitation at 395 nm). The compositions of the mobile phases were the same as described above. The 267.5 min gradient program was used to compare the non-porous column with the wide-pore column. The gradient elution was 16% B held over 5 min, to 25% in 10 min, to 43% B in 112.5 min, to 45% B in 135 min, to 55% B in 185 min, to 65% B in 215 min, and to 100% B in 267.5 min. The 535 min gradient program was used for proteomics analysis of mitochondrial proteins in livers of the hepatitis-infected mouse model. The gradient elution was 16% B held over 10 min, to 25% in 20 min, to 43% B in 225 min, to 45% B in 270 min, to 55% B in 370 min, to 65% B in 430 min, and to 100% B in 535 min. To keep the long life-time of the non-porous column, a washing operation was performed after operation of each analysis. The gradient time program of the washing operation was 100 to 0% B in 5 min and 0 to 100% B in 10 min at 0.3 mL/min of flow rate, which was repeated four times.

The isolated derivatized proteins were identified as reported in Ref. [5] using HPLC and tandem mass spectrometry. The obtained amino acids sequence data were searched for the taxonomy *Mus musculus* against the National Center for Biotechnology Information non-redundant (NCBInr) database using MASCOT version 2.1.03 (Matrix Science, Ltd., London, UK).

3. Result

3.1. Separation of DAABD-calcitonin in gradient elution with the non-porous column

The non-porous column was applied to separate fluorogenic derivatized calcitonin, a model peptide, to investigate its separation efficiency. Calcitonin (0.5 μM, M.W. 3418) was derivatized with a fluorogenic reagent, 7.0 mM DAABD-Cl, and subjected to HPLC-fluorescence detection in gradient elution on either the non-porous or the wide-pore column. Both columns were the same size (4.6 i.d. × 250 mm). The retention times and shapes of both DAABD-calcitonin peaks suggested that the non-porous column exhibited stronger affinity for the peptide and higher resolution than the wide-pore column (Fig. 2). The retention time of the compounds less retained on the non-porous column was shorter than that on the wide-pore column. The separation efficiencies of both columns were then compared utilizing the peak capacity, since the separation efficiency of HPLC columns in gradient elution is usually evaluated with column peak capacity P, while under isocratic conditions it is evaluated with theoretical plates N. The peak capacity represents the maximum theoretical number of components that can be separated in a column within a given gradient time. Each P value was then calculated from peak width w measured at 4σ

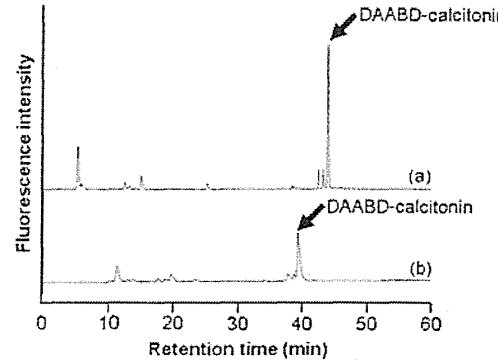

Fig. 2. Chromatograms obtained from DAABD-calcitonin separated in (a) the non-porous column or (b) the wide-pore column under gradient elution conditions. Chromatographic conditions are described in Section 2.

(13.4% of peak height) and the gradient time t_g according to Eq. (1) [12]:

$$P = 1 + \frac{t_g}{w} \quad (1)$$

The P value with the non-porous column was found to be threefold higher than that with the wide-pore column under 60 min gradient conditions (197 with the non-porous column vs. 64 with the wide-pore column). In a similar experiment using a typical standard protein (β-lactoglobulin, M.W. 18,363), the P value exhibited the same tendency with both columns (data not shown). These results indicate that separation efficiency in the non-porous column was superior to that in the wide-pore column.

3.2. Optimized column length and flow rate with the non-porous column

In order to obtain appropriate separation efficiency, the gradient elution of DAABD-calcitonin was performed with different lengths (50, 100, 150, and 250 mm) of the non-porous column at different flow rates (0.2, 0.3, 0.4, and 0.5 mL/min). However, for the 250 mm-long column, the flow rate was limited to a maximum of 0.3 mL/min because of the durability of the HPLC flow (20 MPa) system used in the present experiment. DAABD-calcitonin was separated in the same 60 min gradient program as described in Section 3.1, and each P value was calculated according to Eq. (1). The P value increased with increasing column length and flow rate, indicating that separation efficiency was greater with a longer column and a higher flow rate (Fig. 3A). The same was true for β-lactoglobulin, a model protein (data not shown).

Moreover, mitochondrial protein extract was injected into each length of the columns at the maximum flow rate (0.3 or 0.5 mL/min) to investigate the separation of a real biological sample. The number of separated protein peaks increased with increasing column length: a 250 mm-long column at a 0.3 mL/min flow rate exhibited the highest separation efficiency for the actual protein mixture sample (Fig. 3B). Therefore, a column length of 250 mm with a flow rate of 0.3 mL/min was selected for separating the mitochondrial protein extract.

3.3. Comparison of the non-porous column with the wide-pore column for separating a mitochondrial protein extract

Based on the results above, the non-porous column (250 mm length with a flow rate of 0.3 mL/min) was applied to separate a mitochondrial protein extract. The chromatogram obtained under the appropriate conditions described in Section 2.5 was compared with that obtained from the wide-pore column (250 mm length,

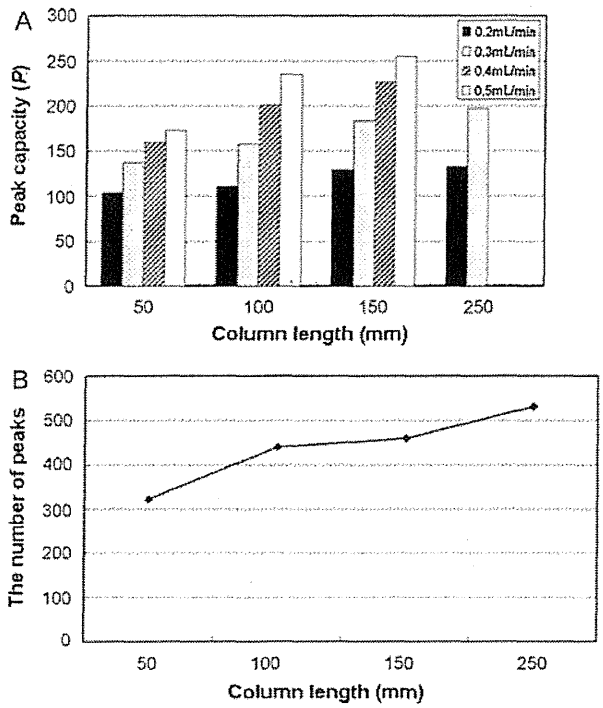

Fig. 3. (A) Peak capacities of the non-porous column with various column lengths (50, 100, 150, and 250 mm) at various flow rates (0.2, 0.3, 0.4, and 0.5 mL/min) in the gradient elution of DAABD-calcitonin. Each P value was calculated with Eq. (1) in Section 3.2. (B) The number of protein peaks separated in each length of the column (50, 100, 150, and 250 mm) obtained from the mitochondrial protein extract. The flow rate was 0.5 mL/min, except for the 250 mm column that had a 0.3 mL/min flow rate. The details are described in Section 2.

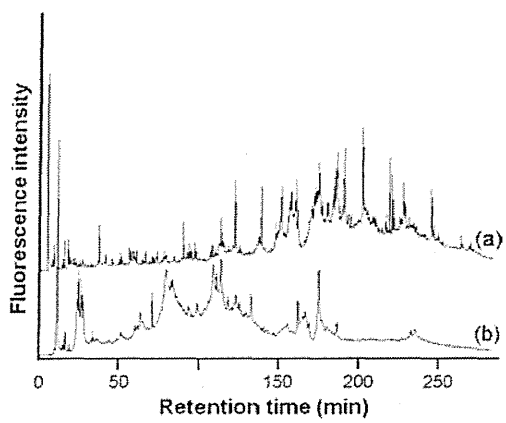

Fig. 4. Chromatograms of mouse liver mitochondrial proteins separated in (a) the non-porous column or (b) the wide-pore column. Chromatographic conditions are described in Section 2.

0.3 mL/min). Fig. 4a indicates that 420 protein peaks were obtained on the chromatogram with the non-porous column in 260 min analytical time. However, 160 protein peaks were not clearly separated in the chromatogram with the wide-pore column (Fig. 4b). This result clearly suggested that the non-porous column, rather than the wide-pore column, would be useful for proteomics analysis of mouse liver mitochondrial proteins with the FD–LC–MS/MS method.

Also, the retention times and peak shapes of the proteins injected into the non-porous column exhibited stronger adsorption and higher resolution than those injected into the wide-pore column. Furthermore, the retention time of the compounds less

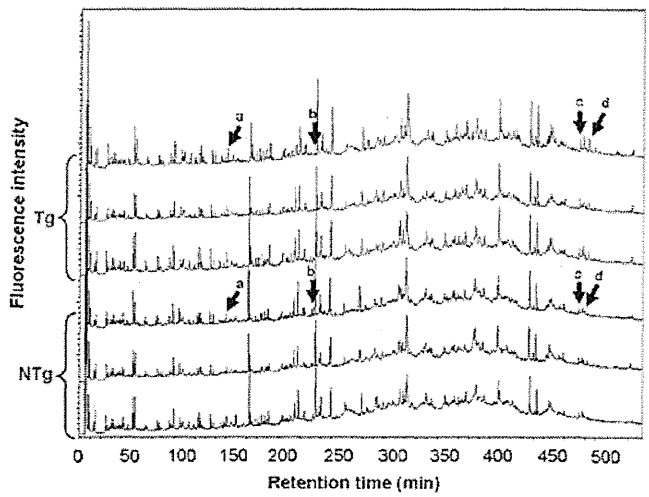

Fig. 5. Chromatograms of liver mitochondrial proteins in Tgs (red) and NTgs (blue) mice separated in the non-porous column. The peaks indicated by arrows fluctuated between Tgs and NTgs. Chromatographic conditions are described in Section 2. (For interpretation of the references to color in this figure legend, the reader is referred to the web version of the article.)

retained in the non-porous column was shorter than that on the wide-pore column.

3.4. Proteomics analysis of mitochondrial proteins in livers of hepatitis-infected mouse model

Differential proteomics analysis was performed on the non-porous column between mitochondrial protein samples extracted from livers of Tgs ($n=3$) and NTgs ($n=3$) mice aged 16 months. This age was selected based on the previous report that many proteins related to the function of mitochondrial events fluctuated in Tg. The appropriate separation conditions in HPLC afforded 500 protein peaks on each chromatogram for Tgs and NTgs in 9 h of analysis (Fig. 5), with each peak height representing the amount of each protein. The responsibility of this analysis was confirmed, based on the reproducibility of the retention times and the peak heights. The relative standard deviations (RSDs) of peaks a through d (Fig. 5) ranged from 0.0 to 0.5% for retention times and 0.4–18.0% for peak heights (for between-days, $n=3$–6). The heights of peaks corresponding to specific retention times were compared between Tgs and NTgs. The expression of several peaks fluctuated, and each fluctuating peak fraction was collected, digested, and subjected to LC–MS/MS analysis to identify the protein. Table 1 summarizes the identified proteins. Three proteins were significantly up-regulated ($Tg/NTg = 1.24$–2.86, $0.05 \leq p < 0.10$) (Peaks a, c, and d in Fig. 5) in Tg, while one protein peak was significantly down-regulated ($Tg/NTg = 0.44$, $p < 0.05$) (Peak b in Fig. 5). Those four proteins were demonstrated for the first time in liver mitochondrial proteomics analysis.

4. Discussion

4.1. Comparison of the separation of DAABD-calcitonin and DAABD-β-lactoglobulin between the non-porous column and the wide-pore column

In order to determine the difference in separation between the non-porous column and the wide-pore column, a derivatized model peptide and protein (DAABD-calcitonin and DAABD-β-lactoglobulin) were separated. The retention times of the derivatized model samples were longer for the non-porous col-

Table 1
Differentially expressed liver mitochondrial proteins between Tgs and NTgs.

Peak number	Tg/NTg ratio		Protein name	Accession number	Score	Sequence coverage (%)
a	1.24	± 0.17	60S ribosomal protein L11	gi 13385408	129	12
b	0.44	± 0.33	Sterol-carrier protein 2	gi 45476581	278	10
c	1.51	± 0.35	NADH-cytochrome b5 reductase 3	gi 19745150	145	8
d	2.86	± 1.30	Hydroxysteroid (17-beta) dehydrogenase 13	gi 159573879	183	25

umn than for the wide-pore column. Since the surface of the non-porous column is covered with ODS (C18) and the surface of the wide-pore column consists of a less hydrophobic "reversed-phase" ligand than C18, stronger retention of the derivatized model samples should be caused by the hydrophobic interaction in the non-porous column. In contrast, considering the shortest retention times of the hydrophilic substances, the non-porous column should exhibit fewer void volumes than the wide-pore column. It was also shown that, considering the *P* (peak capacity) value for the non-porous column was threefold higher than that for the wide-pore column, the non-porous and small size (2 μm as compared to 3 μm of the wide-pore column) reduced eddy diffusion and mass-transfer resistance on separation and resulted in high-resolution chromatography [8]. This couldn't be caused by the narrow particle size distribution of the former column since the particle size distribution of both the columns were similar (D90/D10 < 1.4, and D90/D10 = 1.42 for the non-porous and the wide-pore, respectively, measured by laser diffraction particle size analysis and electrical sensing zone method).

4.2. Optimization of column length and flow rate for protein separation with the non-porous column

The effects of column length and flow rate on the *P* value were investigated using DAABD-calcitonin and DAABD-β-lactoglobulin to obtain optimal conditions for derivatized protein separation on the non-porous column. High *P* values were obtained using a longer column and a higher flow rate. This tendency agreed with the simulation of separation efficiency reported by Gilar et al. [12], indicating that the length of the non-porous column was proportional to separation efficiency. In this study, 0.3 mL/min was the maximum flow rate for the longest column (250 mm) because of the currently limited operating pressure (20 MPa). The LC system should be mechanically strong enough to withstand the ultrahigh pressures for further efficient separation in the non-porous Presto FF-C18 that might be 250 mm long and have a flow rate exceeding 0.3 mL/min. In this sense, in the future, further efficient separation should be examined utilizing an Ultra High Pressure Liquid Chromatography system. According to the results (Fig. 3A), the highest *P* value was obtained with a 150 mm length of column and a flow rate of 0.5 mL/min. However, more separated proteins were observed in the 250 mm-long column with a 0.3 mL/min flow rate for the mitochondrial sample (Fig. 3B). This is because the separable peaks from a large numbers of proteins in a real biological sample should be proportional to the column length. Another reason is that the dilution of the peak fraction in a 150 mm column with a high flow rate of 0.5 mL/min might be beyond the detection limit of the system. Therefore, a 250 mm column length with a flow rate of 0.3 mL/min was adopted as the optimal condition for separating liver mitochondrial proteins.

4.3. Application of the FD–LC–MS/MS method using the non-porous column for differential proteomics analysis of liver mitochondria

Nine hours of analysis indicated that the number (500) of mitochondrial protein peaks (Fig. 5) was similar to the number of extracted proteins from a whole cell separated with the wide-pore column (e.g., for mouse liver proteomics analysis) [4]. Concerning the life-time of the non-porous column, the life-time was long enough to analyze mitochondrial proteins about 40 times (400 h including the washing period) since the chromatogram obtained after 40 times analyses was the same as the initial one. That would be caused by the contribution of a washing operation after each analysis. This result suggests that the non-porous column could be substituted for the wide-pore column as a protein separation column for the FD–LC–MS/MS method.

Compared to the low reproducibility for the retention times of peaks in the previous report [9], the present differential proteomics analysis of liver mitochondria obtained reproducible retention times and peak heights (RSD less than 0.5% for retention times and less than 18.0% for peak heights). The reason for this superior reproducibility may be that in the FD–LC–MS/MS method, proteins were derivatized with the hydrophilic reagent and a low amount of proteins. These results indicate that the FD–LC–MS/MS method using the non-porous column can be used for differential proteomics analysis of liver mitochondria and results in identification of four fluctuating proteins between Tgs and NTgs.

4.4. Functions of the fluctuating liver mitochondrial proteins related to hepatocarcinogenesis

All the identified mitochondrial proteins in this study were demonstrated for the first time in liver proteomics analysis. Since mitochondria were extracted from mouse liver and analyzed for expression of proteins, it is assumed that the proteins inside the mitochondria were concentrated to a detectable level of each expression fluctuation.

Only one down-regulated peak in Tg was identified as sterol carrier protein 2 (SCP2), considering differences in localization between the deduced different types (SCP2 and SCPx) (reviewed in ref. [13]). SCP2 is related to intracellular lipid transport (e.g., cholesterol) from other intracellular membranes to mitochondria [14], as well as from the outer to the inner mitochondrial membrane for oxidation. Since lipids have accumulated in the hepatocytes of 16-month-old Tg mice, causing steatosis as previously reported [10], lipid transport to mitochondria might no longer be required. Thus, SCP2 was decreased in Tg through a negative feedback pathway. Also, SCP2 is reportedly involved in regulation of the signal pathway for lipids (reviewed in ref. [13]). These findings suggest that the decrease of SCP2 in Tg may suppress lipid transport to mitochondria, leading to inhibition of lipid signaling. In contrast, three proteins were demonstrated to be up-regulated in Tg. Hydroxysteroid (17-beta) dehydrogenase 13 (17βHSD13) is specifically expressed in liver [15]. It has been reported that the intracellular localization of 17βHSD13 is similar to that of HCV core protein in endoplasmic reticulum (ER), lipid droplets (LDs), and mitochondria [16–18], while it is unknown whether 17βHSD13 localizes in mitochondria or not. In general, 17βHSD family proteins catalyze the dehydrogenation reactions of the steroid skeleton with an excess of NADH or electrons. Although 17βHSD13 may play a key role in the next step of detoxification and/or utilization of lipid metabolites through the reaction, its specific substrate is not identified. At least, the increase of 17βHSD13 in Tgs would acti-

vate lipid metabolism. NADH-cytochrome b5 reductase 3 (CYB5R3) was observed in the plasma membrane, mitochondrial outer membrane, and ER. CYB5R3 in the mitochondrial electron-transfer system catalyzes the oxidation of NADH to NAD^+ (reviewed in Ref. [19]). For mitochondrial dysfunction, CYB5R3 is up-regulated due to an increase of the NADH/NAD^+ ratio, resulting in enhanced oxidation of NADH to NAD^+. Thus, an increase of CYB5R3 in Tg would accelerate aerobic respiration in mitochondria. In addition, 60S ribosomal protein L11 (RPL11) is associated with Mdm2, which is an E3 ligase for promoting p53 ubiquitination, resulting in prevention of the degradation of p53 [20,21]. The undegraded p53 in mitochondria reportedly causes apoptosis of cancer cells [22,23]. This finding suggests that up-regulated RPL11 would suppress the growth of hepatocarcinoma in transition out of hepatitis C. If hepatocarcinogenesis activates metabolism in Tg mice at the age of 16 months, 17βHSD13 and CYB5R3 might increase and accelerate lipid metabolism and aerobic respiration. Furthermore, a decrease of SCP2 might control lipid transport to mitochondria and thus maintain equilibrium through a negative feedback pathway. Considering these results, fluctuation of these proteins suggests that activation and suppression of hepatocarcinogenesis occur simultaneously in Tg mice at 16 months of age.

In conclusion, a novel non-porous column (Presto FF-C18) achieved good separation of liver mitochondrial proteins, which was hardly achieved on a wide-pore column such as Intrada WP-RP. Moreover, the FD–LC–MS/MS method with Presto FF-C18 demonstrated for the first time several fluctuating proteins performing differential proteomics analysis of liver mitochondrial proteins in a hepatitis-infected mouse model.

References

[1] H.J. Issaq, J. Blonder (Eds.), J. Chromatogr. B: Analyt. Technol. Biomed. Life Sci. Netherlands (2009) 1222.
[2] M. Masuda, H. Saimaru, N. Takamura, K. Imai, Biomed. Chromatogr. 19 (2005) 556.
[3] T. Ichibangase, H. Saimaru, N. Takamura, T. Kuwahara, A. Koyama, T. Iwatsubo, K. Imai, Biomed. Chromatogr. 22 (2008) 232.
[4] T. Ichibangase, K. Moriya, K. Koike, K. Imai, J. Proteome Res. 6 (2007) 2841.
[5] K. Imai, T. Ichibangase, R. Saitoh, Y. Hoshikawa, Biomed. Chromatogr. 22 (2008) 1304.
[6] H. Asamoto, T. Ichibangase, K. Uchikura, K. Imai, J. Chromatogr. A 1208 (2008) 147.
[7] T. Ichibangase, K. Imai, J. Proteome Res. 8 (2009) 2129.
[8] N. Wu, Y. Liu, M.L. Lee, J Chromatogr A, Netherlands (2006) 142.
[9] B.E. Chong, D.M. Lubman, F.R. Miller, A.J. Rosenspire, Rapid Commun. Mass Spectrom. 13 (1999) 1808.
[10] K. Moriya, H. Yotsuyanagi, Y. Shintani, H. Fujie, K. Ishibashi, Y. Matsuura, T. Miyamura, K. Koike, J. Gen. Virol. 78 (Pt 7) (1997) 1527.
[11] M.F. Lopez, B.S. Kristal, E. Chernokalskaya, A. Lazarev, A.I. Shestopalov, A. Bogdanova, M. Robinson, Electrophoresis 21 (2000) 3427.
[12] M. Gilar, A.E. Daly, M. Kele, U.D. Neue, J.C. Gebler, J. Chromatogr. A 1061 (2004) 183.
[13] F. Schroeder, B.P. Atshaves, A.L. McIntosh, A.M. Gallegos, S.M. Storey, R.D. Parr, J.R. Jefferson, J.M. Ball, A.B. Kier, Biochimica Et Biophysica Acta-Mol. Cell Biol. Lipids 1771 (2007) 700.
[14] G.G. Martin, H.A. Hostetler, A.L. McIntosh, S.E. Tichy, B.J. Williams, D.H. Russell, J.M. Berg, T.A. Spencer, J. Ball, A.B. Kier, F. Schroeder, Biochemistry 47 (2008) 5915.
[15] Y. Horiguchi, M. Araki, K. Motojima, Biochem. Biophys. Res. Commun. 370 (2008) 235.
[16] K. Moriya, H. Fujie, Y. Shintani, H. Yotsuyanagi, T. Tsutsumi, K. Ishibashi, Y. Matsuura, S. Kimura, T. Miyamura, K. Koike, Nat. Med. 4 (1998) 1065.
[17] R. Suzuki, S. Sakamoto, T. Tsutsumi, A. Rikimaru, K. Tanaka, T. Shimoike, K. Moriishi, T. Iwasaki, K. Mizumoto, Y. Matsuura, T. Miyamura, T. Suzuki, J. Virol. 79 (2005) 1271.
[18] B. Schwer, S.T. Ren, T. Pietschmann, J. Kartenbeck, K. Kaehlcke, R. Bartenschlager, T.S.B. Yen, M. Ott, J. Virol. 78 (2004) 7958.
[19] R. de Cabo, E. Siendones, R. Minor, P. Navas, Aging (Albany NY) 2 (2010) 63.
[20] K. Itahana, H. Mao, A.W. Jin, Y. Itahana, H.V. Clegg, M.S. Lindstrom, K.P. Bhat, V.L. Godfrey, G.I. Evan, Y.P. Zhang, Cancer Cell 12 (2007) 355.
[21] S. Fumagalli, A. Di Cara, A. Neb-Gulati, F. Natt, S. Schwemberger, J. Hall, G.F. Babcock, R. Bernardi, P.P. Pandolfi, G. Thomas, Nat. Cell Biol. 11 (2009) 501.
[22] N.D. Marchenko, A. Zaika, U.M. Moll, J. Biol. Chem. 275 (2000) 16202.
[23] M. Mihara, S. Erster, A. Zaika, O. Petrenko, T. Chittenden, P. Pancoska, U.M. Moll, Mol. Cell 11 (2003) 577.

SCIENTIFIC REPORTS

SUBJECT AREAS:
EXPRESSION SYSTEMS
BIOLOGICAL TECHNIQUES
GENE DELIVERY
GENE THERAPY

Received
17 November 2012

Accepted
27 December 2012

Published
25 January 2013

Correspondence and requests for materials should be addressed to Y.K. (kanegae@ims.u-tokyo.ac.jp)

* Current address: Japan Animal Referral Medical Center, 2-5-8 Kuji, Takatsu-ku, Kawasaki-shi, Kanagawa 213-0032, Japan.

Efficient production of adenovirus vector lacking genes of virus-associated RNAs that disturb cellular RNAi machinery

Aya Maekawa, Zheng Pei, Mariko Suzuki, Hiromitsu Fukuda*, Yohei Ono, Saki Kondo, Izumu Saito & Yumi Kanegae

Laboratory of Molecular Genetics, Institute of Medical Science, University of Tokyo, Minato-ku, Tokyo, Japan.

First-generation adenovirus vectors (FG AdVs) are widely used in basic studies and gene therapy. However, virus-associated (VA) RNAs that act as small-interference RNAs are indeed transcribed from the vector genome. These VA RNAs can trigger the innate immune response. Moreover, VA RNAs are processed to functional viral miRNAs and disturb the expressions of numerous cellular genes. Therefore, VA-deleted AdVs lacking VA RNA genes would be advantageous for basic studies, both *in vitro* and *in vivo*. Here, we describe an efficient method of producing VA-deleted AdVs. First, a VA RNA-substituted "pre-vector" lacking the original VA RNA genes but alternatively possessing an intact VA RNA region flanked by a pair of FRTs was constructed. VA-deleted AdVs were efficiently obtained by infecting 293hde12 cells, which highly express FLP, with the pre-vector. The resulting transduction titers of VA-deleted AdVs were sufficient for practical use. Therefore, VA-deleted AdVs may be substitute for current FG AdV.

E1- and E3-deleted adenovirus vectors (AdVs) developed in the middle of 1990's[1,2] are commonly known as first-generation (FG) AdVs, and have been extensively used not only for the basic studies of various gene functions *in vitro* and *in vivo* but also for preclinical and clinical gene therapy. Because FG AdVs lack E1A gene, which is an essential transactivator in all other viral promoters driven by RNA polymerase II. Therefore, FG AdVs were usually considered that they do not express any viral gene products. However, FG AdVs, in fact, express VA RNAs that are transcribed by RNA polymerase III when using these vectors both *in vitro* and *in vivo*, because its activity is probably independent of RNA polymerase II.

VA RNAs, VAI and VAII, located at about 30 map units on adenovirus 5 (Ad5), are non-coding RNAs consisting of 157–160 nucleotides (nt). These VA RNAs are extremely abundant during the late phase of infection and inhibit cellular RNA-interference pathways by saturating Exportin 5 and Dicer[3]. Also, VAI inhibits protein kinase R (PKR) activity and, consequently, eliminates the block of the cellular translation machinery to allow the efficient production of viral proteins. Moreover, VA RNAs were processed and generate miRNAs[4,5], known as mivaRNAI and mivaRNAII that disturb the expression of many cellular genes, with the probable result of blocking cellular antiviral machinery. Therefore, there is no doubt that the AdVs lacking VA RNA genes are superior to current FG AdVs.

VAI and VAII are also transcribed not only during the early phase of Ad5 but also in E1A-deleted FG AdV. An E1-containing Ad5 mutant virus is reported which lack the expressions of both VAI and VAII and can proliferate in human cells, but its titers are approximately 60-fold lower than that of wild-type Ad5[6]. Therefore, VA RNAs are not essential, but play an important role in efficient viral growth by overcoming cellular antiviral machinery. Although the E1-containing mutant virus lacking expression of VA RNAs can slightly grow, efficient systems for producing E1-, E3- and VA-deleted AdVs (simply denoted VA-deleted AdVs) are extremely difficult to develop. One system for generating VA-deleted AdV expressing GFP using a 293 cell line that inducibly expresses the VAI gene has been reported[7]. However, the transduction titer produced using this system is approximately 1,000-fold lower than that of current FG AdVs. Furthermore, 18 days (including a secondary passage) are required before VA-deleted AdV are first observed, and the aid of expression markers, such as GFP or luciferase fluorescence, may be necessary to isolate the VA-deleted AdV. Therefore, this production system using a VA-expressing cell line is impractical for general use.

We hypothesized that, although VA RNAs are not essential for viral growth, VA-deleted AdV cannot grow during the initial step of vector generation, where only a few copies of the viral genome are present per cell, possibly because viral genes other than VA RNAs that block the cellular antiviral machinery may not be